

Article

Application of the Analysis Time Series and Multispectral Images for the Estimation of the Conditions of the Vegetation Covers of the Natural Areas of Southern Spain

Federico Benjamín Galacho-Jiménez *, Pablo Quesada-Molina, David Carruana-Herrera  and Sergio Reyes-Corredera 

Geographic Analysis Group, Department of Geography, University of Malaga, 29071 Málaga, Spain

* Correspondence: fbgalacho@uma.es; Tel.: +34-952132172

Abstract: It has been scientifically proven that climate change is a reality. In subarid Mediterranean climates, this fact is observed in the irregular distribution of rainfall, resulting in alternating periods of more or less prolonged drought with episodes of torrential rains concentrated in short periods of time. We have selected 11 natural areas in southern Spain, where we will observe these circumstances and where a series of ecosystems composed of vegetation covers of a high ecological value are found. We start from the question of whether these climatic circumstances are really deteriorating them. For this study, we propose a method that combines three analysis techniques: the design of the time series, the application of vegetation indices, and the use of techniques analysis of changes in land use. From the combination of these techniques in the period from 1997 to 2021, we have observed that there have been a dynamic of changes in land use that has maintained its original characteristics by more than 70%, so it is possible to affirm that the adaptation of ecosystems to climatic conditions has occurred satisfactorily. However, this general statement shows some particularities which are those that we will show in this work.



Citation: Galacho-Jiménez, F.B.; Quesada-Molina, P.; Carruana-Herrera, D.; Reyes-Corredera, S. Application of the Analysis Time Series and Multispectral Images for the Estimation of the Conditions of the Vegetation Covers of the Natural Areas of Southern Spain. *Land* **2023**, *12*, 42. <https://doi.org/10.3390/land12010042>

Academic Editors: David Rodríguez-Rodríguez and Javier Martínez-Vega

Received: 29 November 2022

Revised: 16 December 2022

Accepted: 19 December 2022

Published: 23 December 2022



Copyright: © 2022 by the authors. Licensee MDPI, Basel, Switzerland. This article is an open access article distributed under the terms and conditions of the Creative Commons Attribution (CC BY) license (<https://creativecommons.org/licenses/by/4.0/>).

Keywords: subarid Mediterranean climates; natural areas; time series; vegetation indices; land-use changes; GIS; remote sensing; MODIS

1. Introduction

The biogeographical areas and their ecosystems of southern Europe, specifically the Mediterranean, have been suffering persistent meteorological droughts, torrential rains concentrated in short periods of time [1–5], episodes of extreme temperatures [6,7], and changes in climatic conditions that have become increasingly accelerated and recurrent during the most recent decades [8–14], phenomena that are attributed to climate change [15–20]. The characteristics acquired by these episodes have serious consequences for the ecosystems of natural areas in general, and their vegetation covers in particular. Their response to these conditions is observed in how they endure them [21–26]. Therefore, we believe that it is essential to know the response of ecosystems to different hydrological and meteorological stresses, which can be valuable information for those responsible for the management of these spaces and for researchers in general [27–30]. In which case it will be necessary to propose appropriate measures for the minimization of the effects of the aforementioned phenomena.

In this context, we start from the hypothesis that the ecosystems of the natural areas of southern Spain are differentially supporting climatic conditions, mainly focusing on the precipitation variable, being able to be very vulnerable to the different hydrological and meteorological stresses that climate change is imposing [31–34], a situation that, on the other hand, is being observed in the ecosystems of many other areas worldwide [35–39].

The objective of this work is to evaluate how natural areas are changing in the face of the impact of the climatic conditions imposed by global change, mainly in our case, with special reference to the availability of precipitation and its sequencing. The managers of

these areas are forced to face the challenge of knowing this dynamic to design monitoring programs that allow a rapid assessment of the effects of environmental changes and ecosystem conditions. Therefore, the reduction in the environmental and ecological values that justify its valuation as a natural space and, in most cases, its protection of areas for the preservation of particular and valuable ecosystems, must be considered with the utmost urgency, since we would be talking about attending a relevant and contrasted fact. To alleviate this situation, we think it is essential to work to establish the management actions that would make it possible to maintain the conditions that led to its high valuation and, where appropriate, its protection. One way to do this is to be able to have instruments to evaluate with some agility the states of the different areas. With this intention, we have applied a method to evaluate the responses of these ecosystems. Three techniques and several instruments are combined.

First, the time series have been defined considering the precipitation parameters, which shows the evolution and trends of rainfall regimes in the study area, between 1997 and 2021 (25 years), a procedure that has been carried out based on the abundant scientific literature published on the subject [40–43]. The time series model has been made with data from weather stations representing an independent estimate of the contribution of different hydrological stresses and is based exclusively on the observed data [44,45]. For each time series, an analysis is made of the monthly mean values of precipitation and the relevant hydrological stresses at that time [46–48], through the application of multi-scalar drought indices: the Standardized Precipitation Index (SPI) [49]. This index is used for estimating wet or dry condition based on the precipitation variable. It can collect the temporal variation in droughts. The SPI is useful in that it only requires rainfall as an input and especially where temperature data are missing. We have not been able to complete temperature data for the stations we have worked on, mainly when completing a sequence with a minimum of 20 years. This wet or dry condition can be monitored by the SPI on a variety of time scales from sub seasonal to interannual scales [50,51]. We have opted for a 12-month SPI, which is a comparison of the precipitation for 12 consecutive months with the same 12 consecutive months during all the previous years of available data (1997–2021). The SPI at these time scales reflect long-term precipitation patterns. Because these time scales are the cumulative result of shorter periods that may be above or below normal, the longer SPIs tend toward zero unless a specific trend is taking place. However, we have not considered the use of the SPI to characterize droughts but to qualify the precipitation values that have been used in relation to drought periods. This is intended to make an interpretation of the data without relying exclusively on precipitation as a single input variable [52,53].

This analysis of the climatic conditions of precipitation is completed with the data obtained from three vegetation indices: the NDVI (Normalized Difference Vegetation Index), the NDWI (Normalized Difference Water Index), and the EVI (Enhanced Vegetation Index); basing us for its elaboration in multispectral images is the MODIS (Moderate Resolution Imaging Spectroradiometer), what is a key instrument aboard the Terra (originally known as EOS AM-1) and Aqua (originally known as EOS PM-1). Different studies are using satellites, the time-series MODIS NDVI with climate and stocking data [54–57].

The focus here has been on evaluating spectral indices in terms of their sensitivity to the biophysical parameters of the vegetation and external factors affecting the canopy reflectance, mainly those derived from crop nutrition and humidity conditions. In addition, however, it is believed that estimating other parameters produces good results, such as those presented below [58,59]. First, it is worth highlighting the estimation of vegetation vigor based on the chlorophyll content in the leaves, which is an indicator of tree nutrition and its state of photosynthesis. In this sense, the chlorophyll content in the leaf, as the variable most directly related to the values of this index, makes it possible to determine the differences in the state of the health of the leaf. At the same time, it allows for the narrowing of the interpretation that can be made to only those areas with more lush vegetation cover [60–62]. Second, it is important to highlight the water content, either

of the tree canopy or of the plant's context in general. This estimation has been made based mainly on the NDWI and indirectly through the effect of water stress on the leaf area index (LAI) and the chlorophyll content with reference to the NDVIs. Some authors estimate that vegetation indices based on the shortwave infrared bands (the NIR and SWIR) provide good estimates [63]. The application of the NDWI helps as an indicator of potential evapotranspiration since it is related to this vegetation index through the leaf vigor and water stress. It can be observed that some plots that showed a high vigor in the NDVI presented values that predict a certain level of canopy water stress in the NDWI [64,65]. Third, it is interesting to observe the photosynthetically active radiation absorbed by the tree, especially when the leaves are horizontal, and the soil is sufficiently dark [66,67]. Fourth, although indirectly, it is possible to estimate the green biomass that will be determined by the age of the tree and its percentage of green cover, since healthy adult trees show a very clear response, while areas with growing specimens or with a greater water stress show less leaf vigor and a lower canopy lushness [68–73]. Fifth, and bearing in mind that this study is conducted in semi-arid Mediterranean environments, the analysis of the amount of water supplied to the canopy is fundamental, because it is obviously directly related to the vigor of the tree [74–81].

The method is completed with an analysis of the changes in vegetation covers that have occurred over a period of 30 years, from 1991 to 2020. The choice of these dates is justified because the intention is to assess their status in the previous year's closest to those stipulated for the analysis carried out with the time series and vegetation indices (1997–2021), and their comparison with the current situation through the process of the analysis of the changes produced [82–86].

The selection of the best structure of the method is done through a verification based on the reliability criteria [87]. As a result, the spatial variation in the modelled responses and the degree of vulnerability of the ecosystems to the water conditions they have been suffering can be observed [88]. This provides a method that combines scientific rigor with the application of a series of proven technologies: the use of machine learning techniques for the processing of these images and modelling processes [89], multispectral image processing with spatial remote sensing techniques [90–92], and GIS for the management of the information obtained [93–95]. It is specified in a method for aiding decision-making in the management of natural areas [96]. It has been thought that it is possible to address with these techniques and others related the processing of the data currently available for wide spaces, almost in real time to provide information on the issue at hand [97–102].

Since the problem studied is observed in many other biogeographic spaces, this method has been designed with the intention that it can be replicated in any area, thus creating a geoprocessing structure that only requires the loading of data from other areas, although, obviously, it must be reviewed depending on the particularities of the application area.

2. Materials and Methods

2.1. Study Area

The chosen study area or areas have followed a series of criteria that aim to show their relevance through their degree of protection and management, their uniqueness, and their longitudinal geographical distribution, i.e., from west to east, considering the influence of the Föhn effect on their water resources and the development of their natural vegetation and agricultural uses. A total of 11 natural areas are included in this work. In total, they cover an area of 3338 km². See Figure 1 for its location and Table 1 for the surface values.

The selection of the natural areas that we have made responds to the fact that our intention is to observe the precipitation variability in and the spatial distribution of the droughts. Different studies have shown that there is a pattern of rainfall propagation in southern Spain, which goes from west to east in the southern sectors of the Iberian Peninsula [103,104]. The spatial propagation of precipitation also shows the influence of the relief on the space studied, caused by the main mountain systems. According to some

studies, the spatial spread of droughts also shows the effect caused by the main relief features in the space studied [105,106]. In the west, in the province of Cádiz and Málaga and the inland, we find the Serranía de Ronda and the Sierra de las Nieves, where the natural areas of Sierra de Grazalema and Sierra de las Nieves are located; towards the sea, we find the natural areas of Sierra Bermeja and Real, Sierra Blanca, Canucha and Alpujata, and Sierra de Mijas. In the center and extreme east of the province of Malaga, the natural areas of Montes de Málaga, Sierra de Tejeda, Almirajara, Alhama, Sierra de Lújar, Jolúcar, and El Conjuero are located, already in the province of Granada that are configured as medium mountains. Moving eastwards, in the province of Almeria, the mountains are still parallel to the coast with a higher coastal chain where the natural areas of Sierra de Gádor y Enix, Sierra de Filabres, Sierra de Cabrera y Bédar. See Figure 2 to observe the configuration of the relief in the selected areas.

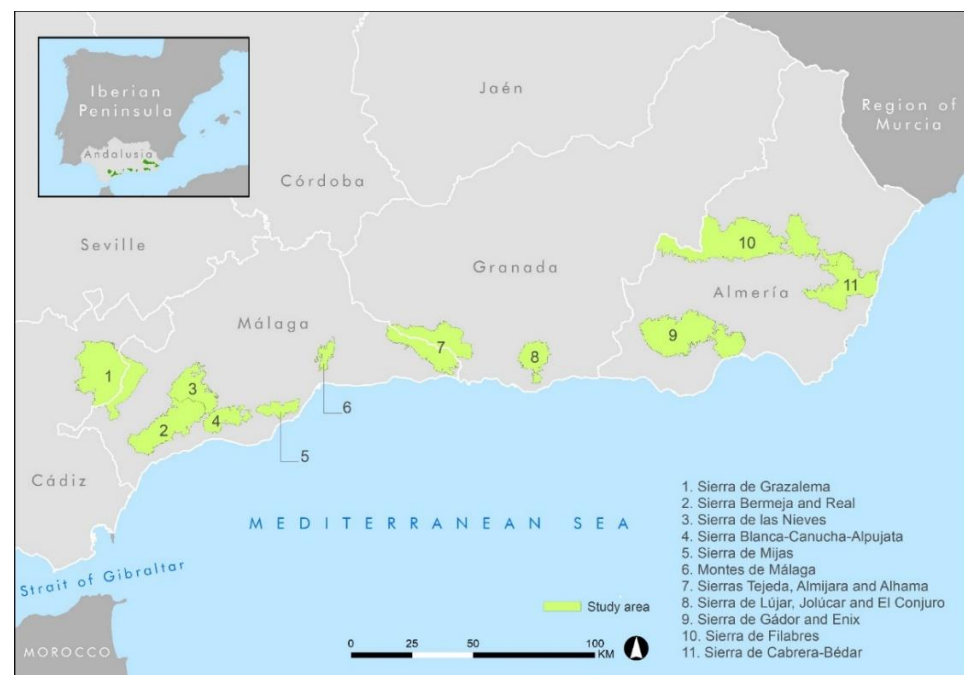


Figure 1. Location of the study area and selected natural areas. Own elaboration based on Basic Spatial Data of Andalusia (DERA). Statistical and Cartographic Institute of Andalusia. Government of Andalusia.

Table 1. Surface and high values of the natural areas.

Natural Areas	Area (km ²)	Average Height (m)	Max. Height (m)	Min. Height (m)
Sierra de Grazalema (SG)	530.4	745.6	1626.2	215.4
Sierras Bermeja and Real (SBR)	289.2	662.6	1475.9	77.6
Sierra de las Nieves (SN)	183.9	1018.8	1901.4	236.7
Sierra Blanca, Canucha, and Alpujata (SBCA)	121.8	639.2	1265.4	118.4
Sierra de Mijas (SM)	78.0	531.1	1139.6	63.0
Montes de Málaga (MM)	49.9	647.4	1028.5	120.2
Sierras de Tejeda, Almirajara, and Alhama (STAA)	400.7	1094.7	2066.6	53.6
Sierra de Lújar, Jolúcar, and El Conjuero (SLJC)	127.1	927.8	1869.0	227.4
Sierra de Gádor and Enix (SGE)	503.1	1186.8	2243.2	51.2
Sierra de Filabres (SF)	716.6	1336.4	2159.3	349.6
Sierra de Cabrera and Bédar (SCB)	337.0	397.4	950.3	2.9
Total Area	3338.1	–	–	–

Own elaboration based on Basic Spatial Data of Andalusia (DERA). Statistical and Cartographic Institute of Andalusia. Government of Andalusia.

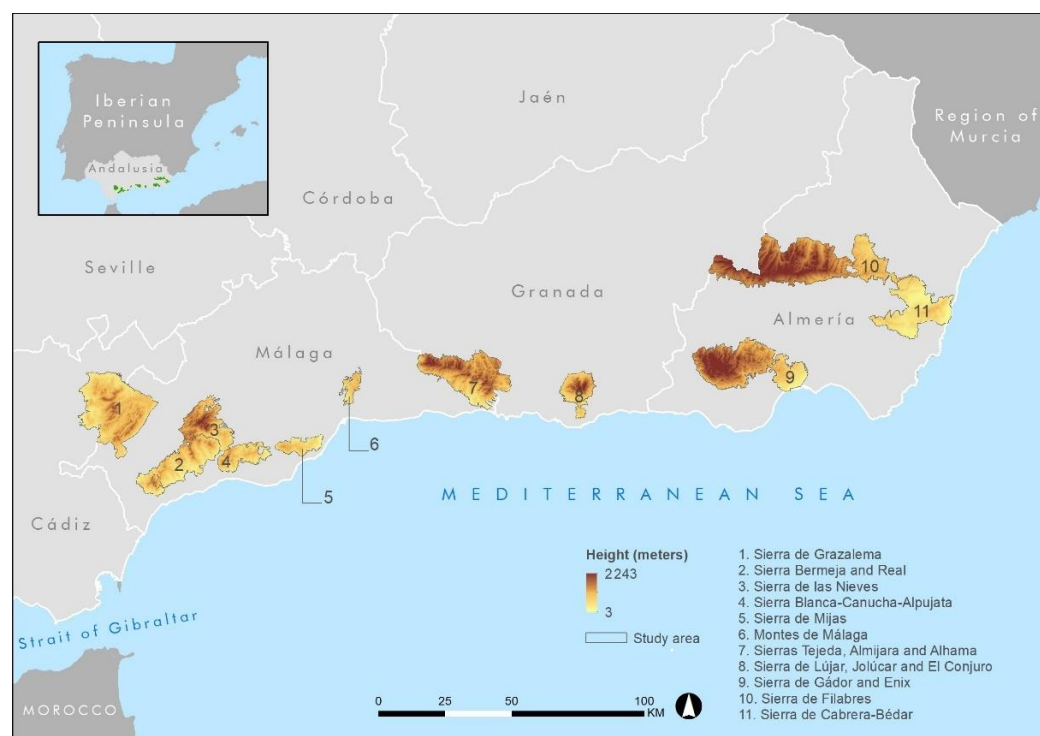


Figure 2. Representation of relief of the study area and selected natural areas. Own elaboration based on Basic Spatial Data of Andalusia (DERA). Statistical and Cartographic Institute of Andalusia. Government of Andalusia.

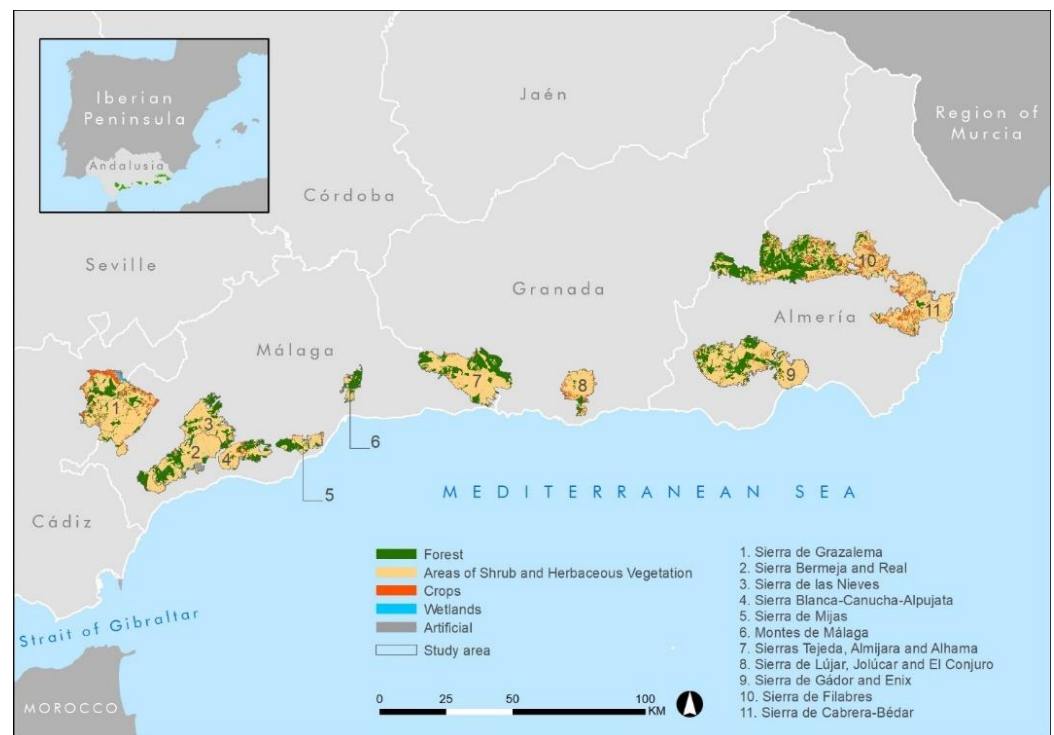
In relation to their degree of protection and management, as natural spaces, in order of relevance, the Sierra de las Nieves National Park stands out, declared in Law 9/2021 of the Spanish state, due to the large floristic inventory (more than 1400 species of plants), of which fifteen species of flora are threatened because they are unique or scarce. This is the case of the Spanish fir or the high mountain gall oak. In addition, the study area includes several Natural Parks: Montes de Málaga, Sierra de Grazalema (Law 2/1989, of 18 July 1989, of the Andalusian regional government), Sierras Tejeda, Almijara, and Alhama (Decree 191/1999, of 21 September 1999, of the Andalusian regional government). All these areas have justified their protection and management on the basis of their flora and/or by constituting a series of functions as a bioclimatic island, fundamentally in the easternmost areas of the study area: Sierra de Cabrera and Bédar, Sierra de Filabres, and Sierra de Gádor and Enix, or by having a series of protective functions for the population, as in the case of Montes de Málaga and its reforestation pine forest in the interest of reducing the historical floods that flooded the city of Málaga.

Prior to the declarations of the protection of these natural areas, there were already a series of areas with a similar figure, the provincial Special Plans for the Protection of the Physical Environment. These were intended to give category to the functions they had, for example, as a buffer or limit to the exacerbated growth of urban pressure, accelerating processes such as erosion that reverted on areas linked to strategic sectors such as the sun and beach tourism: Sierra Blanca, Canucha, and Alpujata, and Sierra de Mijas, or to respect and conserve these transitions between the coastline and areas of greater ecosystemic importance, this is the case of Sierra de Lújar, Jolúcar, and El Conjuero in relation to high mountain areas (Sierra Nevada) or Sierra Bermeja and Real due to the relationship of their plant species adapted to the materials from the Earth's mantle, something that makes them endemic in most cases due to the toxicity of their lithologies for the development of life (the soils derived from peridotite rocks). See Table 2 for the quantification of the surfaces according to the uses considered and Figure 3 for the distribution in the territory.

Table 2. Land uses of natural areas in 2021. Areas (has).

Natural Areas	Forest	ASHV	Crops	Wetlands	Artificial	Other	Total
SG	29,062.20	15,674.74	5570.21	781.61	1001.32	951.11	53,041.19
SBR	13,812.73	13,167.17	266.74	462.96	1139.98	79.13	28,928.70
SN	10,098.47	7804.50	75.39	172.08	223.36	20.50	18,394.30
SBCA	4327.81	6872.73	476.30	67.04	250.84	187.33	12,182.06
SM	4449.76	2183.33	151.81	81.11	419.59	518.85	7804.46
MM	4354.75	288.40	176.17	61.44	94.99	19.86	4995.60
STAA	18,697.38	20,242.87	412.95	287.20	316.84	120.91	40,078.15
SLJC	2294.74	8793.98	1167.81	75.11	246.36	131.90	12,709.90
SGE	17,069.00	31,375.39	906.61	312.97	551.22	97.74	50,312.93
SF	33,794.20	29,879.95	5798.09	383.11	1120.61	689.40	71,665.37
SCB	1366.84	24,552.86	5127.36	397.25	1370.12	889.06	33,703.49
TOTAL	139,327.87	160,835.92	20,129.44	3081.89	6735.22	3705.79	333,816.15

Legend natural areas: SG: Sierra de Grazalema; SBR: Sierra Bermeja and Real; SN: Sierra de las Nieves; SBCA: Sierra Blanca, Canucha, and Alpujata; SM: Sierra de Mijas; MM: Montes de Málaga; STAA: Sierra de Tejeda, Almijara, and Alhama; SLJC: Sierra de Lújar, Jolúcar, and El Conjuero; SGE: Sierra de Gádor and Enix; SF: Sierra de los Filabres; SCB: Sierra de Cabrera and Bédar. Legend land uses: forest, forest areas; ASHV, areas of shrub and herbaceous vegetation; crops, cultivated areas; wetlands, water channels and sheets; artificial, facilities, buildings, and road network with connection to the natural area; other, other areas not included in the above: network of unpaved roads, technical buildings, urban sprawl, etc. Own elaboration based on Geographical Information System for the Identification of Agricultural Land Parcels (SIGPAC). Regional Ministry for Agriculture, Livestock, Fisheries and Sustainable Development. Government of Andalusia.

**Figure 3.** Location of land uses of natural areas in 2021. Own elaboration based on data of the Geographical Information System for the Identification of Agricultural Land Parcels (SIGPAC) (2021).

2.2. Data Source

The time series shall consist of two parameters: the average precipitation as the main parameter and the Standardized Precipitation Index (SPI) as a complementary parameter. For the first parameter, the data of the main database of the network of the stations of the Automatic Hydrological Information System (SAIH) Hidrosur, belonging to the Andalusian Mediterranean Basin of the Autonomous Community of Andalusia. The SAIH Hidrosur

Network began its operation in 1991, having provided data continuously since then. A total of 89 stations with at least 25 years of continuous data have been analyzed for the period between 1997 and 2021. Based on the daily rainfall, the average monthly rainfall for each year and the total annual rainfall have been calculated. The annual precipitation distribution data are shown in Table 3 and the process of assigning the weather stations to each of the protected areas has been carried out through a proximity criterion. It can be seen in Figure 4.

Table 3. Annual distribution of precipitation (L/m²) for each natural space.

Years	Natural Areas										
	SG	SBR	SN	SBCA	SM	MM	STAA	SLJC	SGE	SF	SCB
1997	1080.87	1134.45	908.34	891.25	651.08	723.41	648.89	528.86	313.24	376.91	248.58
1998	632.17	683.83	596.94	597.40	355.88	396.49	353.80	303.14	162.36	185.50	157.24
1999	654.93	683.28	455.24	383.60	246.65	348.93	398.16	391.44	260.67	219.12	194.06
2000	998.33	1140.05	816.72	748.18	469.43	506.31	517.16	523.73	304.57	248.29	230.68
2001	904.63	861.58	738.61	680.83	407.18	546.69	486.44	397.49	261.92	269.39	183.76
2002	843.87	857.10	588.85	574.23	365.75	466.66	515.00	399.45	240.07	250.52	215.10
2003	1044.77	1107.83	912.30	854.53	533.63	736.96	640.38	499.63	319.47	291.06	278.54
2004	647.30	685.00	606.70	611.30	448.63	645.99	499.51	321.11	310.14	331.41	264.76
2005	433.50	494.37	334.51	360.05	202.75	276.97	239.99	181.39	150.86	126.43	166.46
2006	841.57	890.67	712.60	751.33	469.05	551.66	470.96	340.74	292.71	341.04	315.30
2007	746.90	792.08	603.37	626.13	351.25	368.20	372.27	262.38	240.83	254.40	283.12
2008	928.70	979.88	788.18	772.98	439.18	530.40	539.93	433.99	330.46	309.59	250.90
2009	1083.57	1006.35	761.10	726.78	453.13	585.71	658.72	595.96	395.53	293.91	238.12
2010	1533.93	1688.93	1334.25	1434.45	1011.00	876.69	911.83	830.51	554.24	387.31	360.54
2011	859.33	889.58	708.85	769.93	496.58	549.53	520.24	429.64	295.03	272.20	256.12
2012	842.60	795.00	647.54	589.25	554.13	633.13	521.21	387.24	246.33	217.61	312.56
2013	1001.00	912.70	609.01	489.50	328.58	452.83	417.95	354.31	205.72	204.37	156.90
2014	962.30	876.22	630.48	558.63	332.00	444.24	403.89	323.20	194.82	155.36	111.72
2015	582.43	659.30	481.02	434.33	344.83	368.66	323.28	320.07	256.19	242.96	213.78
2016	937.30	1021.48	729.27	721.10	622.33	539.53	403.44	370.00	285.89	262.64	253.12
2017	536.20	572.50	430.08	402.15	337.23	339.77	271.51	260.08	169.01	157.57	186.00
2018	1204.43	1316.48	1041.62	906.43	594.15	661.11	718.55	613.25	374.34	312.26	192.12
2019	568.13	591.17	432.08	389.10	236.48	270.14	294.35	291.00	211.22	273.16	209.38
2020	725.73	658.63	579.95	590.38	562.38	600.99	377.65	292.73	193.83	207.19	191.20
2021	652.87	690.47	390.94	403.25	379.08	371.31	349.54	286.43	256.98	255.37	276.82
Mean	858.15	885.79	673.54	654.31	451.76	514.70	475.17	396.11	276.83	257.46	233.95
STD	247.64	269.49	220.84	234.42	166.41	149.85	158.15	145.39	88.07	62.86	58.71

Legend natural areas: SG: Sierra de Grazalema; SBR: Sierra Bermeja and Real; SN: Sierra de las Nieves; SBCA: Sierra Blanca, Canucha, and Alpujata; SM: Sierra de Mijas; MM: Montes de Málaga; STAA: Sierra de Tejada, Almijara, and Alhama; SLJC: Sierra de Lújar, Jolúcar, and El Conjuero; SGE: Sierra de Gádor and Enix; SF: Sierra de los Filabres; SCB: Sierra de Cabrera and Bédar. Own elaboration based on Automatic Hydrological Information System (SAIH) Hidrosur, Autonomous Community of Andalusia (Spain).

The values reached by the SPI for those same years have been obtained. The ideal is to have a minimum of between 20 and 30 years of monthly values of precipitation, although according to the literature, the optimal would be to have more years [107–109]. The SPI is a powerful and flexible index and is easy to calculate; in fact, the only parameter necessary for its calculation is the precipitation. In addition, it is effective to analyze wet periods and cycles such as dry ones on, which we will rely to determine our time series. The SPI is an index based on a precipitation probabilistic approach. McKee et al. (1995) [49] developed this index with the intention of illustrating the main characteristics of droughts. For its elaboration, the following parameters are taken into consideration: usable water resources including the soil moisture, ground water, snowpack, river discharges, and reservoir storages. The SPI was designed to consider the impact of droughts on these parameters. The soil moisture conditions respond to precipitation anomalies on a scale which is relatively short. Long-term precipitation anomalies are reflected in the waters

underground, river flows, and storage in reservoirs [110]. The SPI data have not been prepared by us but have been obtained through the portal <https://monitordesequia.csic.es/> (accessed on 21 December 2022).

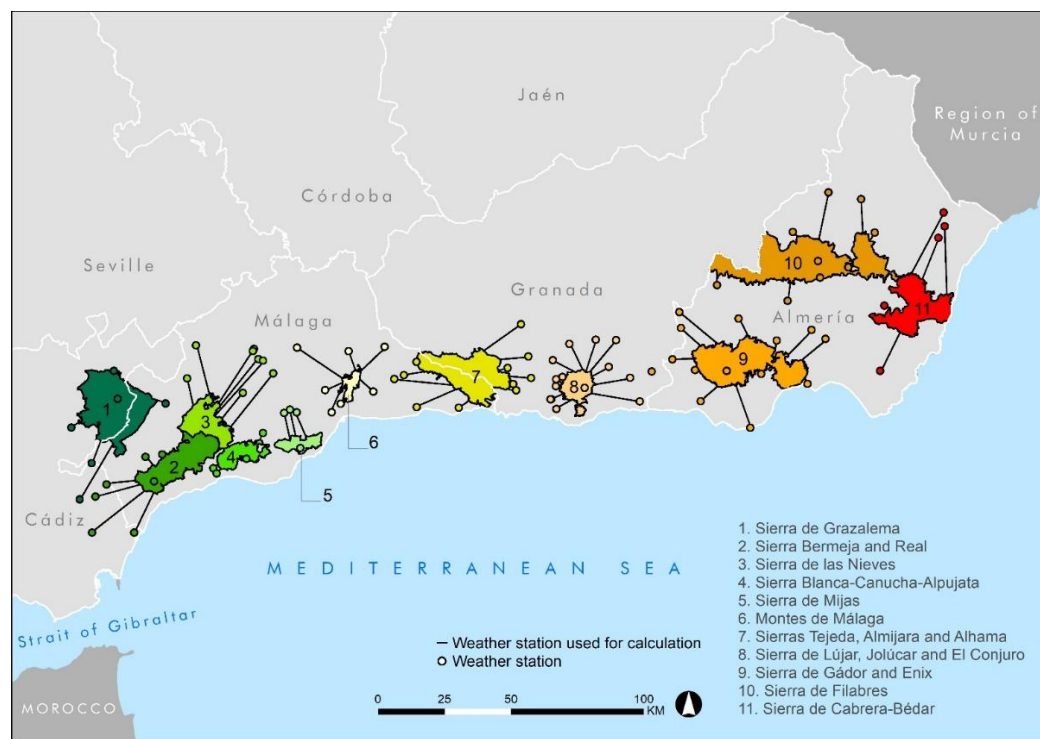


Figure 4. Assignment of weather stations to their corresponding AP according to a criterion of distance or proximity. Own elaboration.

For the calculation of vegetation indices, we have used multispectral images from MODIS. In this case, we used land products that are available through the Land Processes DAAC at the U. S. Geological Survey EROS Data Center (EDC) [<https://lpdaac.usgs.gov/>] (accessed on 21 December 2022).

For the quantification and typification of the different vegetation covers and for the analysis of the changes in vegetation covers, we have used the layers of land use cover which come from two data sources. The date of 1991 has been used as the Cartography of the Uses and Vegetation Covers of the soil of Andalusia of the year 1984 at scale 1:25,000, updated between the years 1988 and 1990. For the data of 2021, we have used the Geographical Information System for the Identification of Agricultural Land Parcels (SIGPAC). The Regional Ministry for Agriculture, Livestock, Fisheries and Sustainable Development, the Government of Andalusia (Spain).

2.3. Method

The method developed has been based on a series of requirements. First, it has been thought that the variables have a tracking capacity, since they are expected to have a relatively short response time so that it can allow for the adaptive management and follow-up and for an early detection of the changes. Second, the establishment of the reference conditions and the range of variability on which to evaluate the changes suffered by ecosystems represents a key aspect for the evaluation of their state of these. Therefore, the variables set out below have been used, and through which the conditions of the vegetation covers are defined in a temporal evolution [111–118]. The applied method follows this process, see Figure 5.

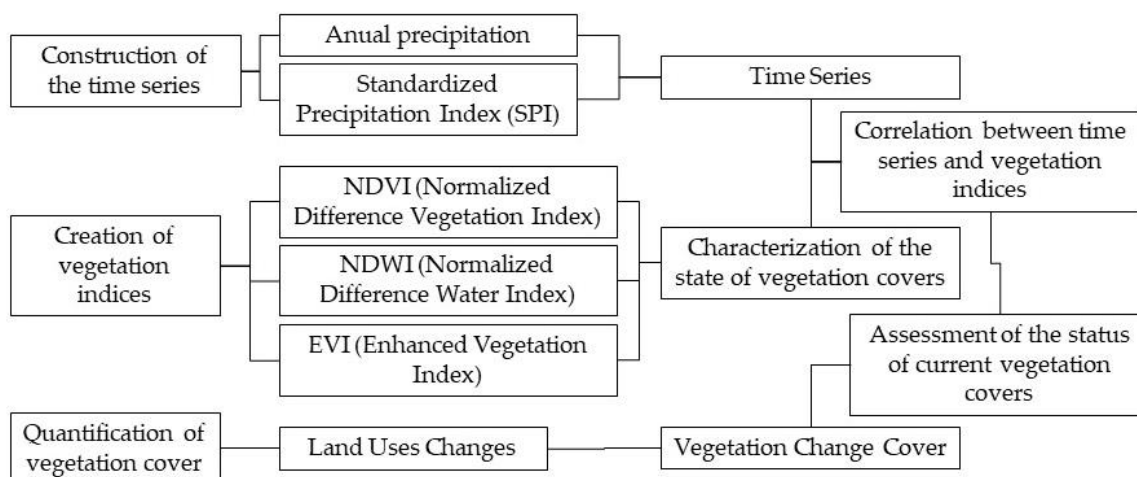


Figure 5. Workflow.

2.3.1. Time Series Design

The time series have been constructed based on precipitation and the SPI. First, the daily precipitation data have been calculated to obtain the monthly averages for each year and then the final average of all the seasons assigned to the same protected area; in this way, we obtain a unique precipitation value for each of the 11 areas. From here, a classification is made based on the values of the data for each year, attempting to know the deviations or anomalies with respect to the average values of rainfall for each area of study. For the construction of the time series, the following process is carried out. Five time series have been established between the years considered (1997–2021): very wet, wet, around average, dry, and very dry years. Each year it is ascribed to a series according to the annual rainfall. For this, the mean and the standard deviation of the data are applied. Data on the mean and standard deviation can be found in Table 3. It is considered that an average year is one where the total volume of precipitation is within the interval that exists between the mean and half of a standard deviation ($x \pm \Phi/2$); a wet year is one that exceeds this interval, being in a value between $x + \Phi/2$ and $x + 3\Phi/2$; similarly, for dry years, simply change the sign so that those between $x - \Phi/2$ and $x - 3\Phi/2$ are considered to be so; finally, very dry years are considered to be those with rainfall totals below $x - 3\Phi/2$ and very wet years are those that show values higher than $x + 3\Phi/2$ [119]. See the results in Tables 4 and 5.

Table 4. Time series (1997–2021). Criteria for category assignment: precipitation volume (L/m²).

Natural Areas	Very Wet	Wet	Mean	Dry	Very Dry
Sierra de Grazalema	>1215.80	1215.80–971.86	971.86–727.92	727.92–483.99	<483.99
Sierras Bermeja and Real	>1290.02	1290.00–1020.53	1020.53–751.05	751.05–481.56	<481.56
Sierra de las Nieves	>1004.82	1004.82–783.97	783.97–563.12	563.12–342.27	<342.27
Sierra Blanca, Canucha, and Alpujata	>997.94	997.94–766.44	766.44–534.93	534.93–303.42	<303.42
Sierra de Mijas	>698.71	698.71–531.36	531.36–364.02	364.02–196.67	<196.67
Montes de Málaga	>740.07	740.07–587.82	587.82–435.57	435.57–283.32	<283.32
Sierras de Tejada, Almirajara, and Alhama	>706.58	706.58–551.65	551.65–396.72	396.72–241.79	<241.79
Sierra de Lújar, Jolúcar, and El Conjuero	>607.46	607.46–467.49	467.49–327.53	327.53–187.56	<187.56
Sierra de Gádor and Enix	>401.95	401.95–316.02	316.02–230.09	230.09–144.16	<144.16
Sierra de Filabres	>356.52	356.52–290.72	290.72–224.92	224.92–159.13	<159.13
Sierra de Cabrera and Bédar	>322.02	322.02–263.31	263.31–204.06	204.06–145.89	<145.89

Source: own elaboration based on Automatic Hydrological Information System (SAIH) Hidrosur, Autonomous Community of Andalusia (Spain).

Table 5. Time series (1997–2021). Assignment of years according to their categorization by the volume of precipitation.

Natural Areas	Series 1	Series 2	Series 3	Series 4	Series 5
	Very Wet	Wet	Mean	Dry	Very Dry
Sierra de Grazalema	2010 (1)	1997/2000/2003/ 2009/2013/2018 (6)	2001/2002/2006/2007/2008/ 2011/2012/2014/2016 (9)	1998/1999/2004/ 2015/2017/2019/ 2020/2021 (8)	2005 (1)
Sierras Bermeja and Real	2010/2018 (2)	1997/2000/2003/ 2016 (4)	2001/2002/2006/2007/2008/ 2009/2011/2012/2013/2014 (10)	1998/1999/2004/ 2005/2015/2017/ 2019/2020/2021 (9)	–
Sierra de las Nieves	2010/2018 (2)	1997/2000/2003/ 2008 (4)	1998/2001/2002/2004/2006/ 2007/2009/2011/2012/2013/ 2014/2016/2020 (13)	1999/2015/2017/ 2019/2021 (5)	2005 (1)
Sierra Blanca, Canucha, and Alpujata	2010 (1)	1997/2003/2008/ 2011/2018 (5)	1998/2000/2001/2002/2004/ 2006/2007/2009/2012/2014/ 2016/2020 (12)	1999/2005/2013/ 2015/2017/2019/ 2021 (7)	–
Sierra de Mijas	2010 (1)	1997/2003/2012/ 2016/2018/2020 (6)	2000/2001/2002/2004/2006/ 2008/2009/2011/2021 (9)	1998/1999/2005/ 2007/2013/2014/ 2015/2017/2019 (9)	–
Montes de Málaga	2010 (1)	1997/2003/2004/ 2012/2018/2020 (6)	2000/2001/2002/2006/2008/ 2009/2011/2013/2014/2016 (10)	1998/1999/2007/ 2015/2017/2021 (6)	2005/2019 (2)
Sierras de Tejeda, Almijara, and Alhama	2010/2018 (2)	1997/2003/2009 (3)	1999/2000/2001/2002/2004/ 2006/2008/2011/2012/2013/ 2014/2016 (12)	1998/2007/2015/ 2017/2019/2020/ 2021 (7)	2005 (1)
Sierra de Lújar, Jolúcar, and El Conjuro	2010/2018 (2)	1997/2000/2003/ 2009 (4)	1999/2001/2002/2006/2008/ 2011/2012/2013/2016 (9)	1998/2004/2007/ 2014/2015/2017/ 2019/2020/2021 (9)	2005 (1)
Sierra de Gádor and Enix	2010 (1)	2003/2008/2009/ 2018 (4)	1997/1999/2000/2001/ 2002/2004/2006/2007/2011/ 2012/2015/2016/ 2021 (13)	1998/2005/2013/ 2014/2017/ 2019/2020 (7)	–
Sierra de Filabres	1997/2010 (2)	2003/2004/2006/ 2008/2009/2018 (6)	2000/2001/2002/2007/2011/ 2015/2016/2019/2021 (9)	1998/1999/2012/ 2013/2020 (5)	2005/2014/2017 (3)
Sierra de Cabrera and Bédar	2010 (1)	2003/2004/2006/ 2007/2012/2021 (6)	1997/2000/2002/2008/2009/ 2011/2015/2016/2019 (9)	1998/1999/2001/ 2005/2013/2017/ 2018/2020 (8)	2014 (1)

Legend: value in brackets shows the number of years in each series. Own elaboration based on Automatic Hydrological Information System (SAIH) Hidrosur, Autonomous Community of Andalusia (Spain).

Second, the SPI data have not been prepared by us but have been obtained through the portal <https://monitordesequia.csic.es/> (accessed on 21 December 2022). Our work has consisted of analyzing the data of this index for the dates of our study and with the same temporality, that is, monthly. With the SPI, we will quantify the precipitation deficit for the established time series, which reflects the impact of drought according to the availability of water resources. This parameter will help us to qualify the volume of precipitation measured and to evaluate its effectiveness on the soil. The SPI data have been taken for each natural area and complement the long-term rainfall record for the period analyzed (1997–2021). In this period, this record is adjusted to a distribution of the probabilities and transformed into a normal distribution so that the SPI mean for each area and the desired period is zero [120,121]. This method is a dimensionless index, and it gives negative and positive values to evaluate the severity of drought and wet conditions, respectively; positive SPI values will indicate that the precipitation is greater than the median, and negative values, which are lower. Drought was classified according to the categories to define the different intensities of drought according to the different SPI values [49,122,123]. See Table 6. Data for the study area are shown in Figure 6 where the calculation is displayed using long-term monthly precipitation data that are fitted to the gamma probability distribution function.

Table 6. Normalized Precipitation Index (SPI) values and drought probability of recurrence.

SPI Values	Category	Recurrence (1)	Severity of the Episode	Drought Class
≥2.0 SPI	Extremely wet	0	0	Wet
1.99 to 1.5	Very wet	0	0	Wet
1.49 to 1.0	Moderately wet	0	0	Wet
0.99 to 0.0	Normal wet	33	1 in 3 years	Mild wet
0.0 to −0.99	Normal dry	33	1 in 3 years	Mild drought
−1.0 to −1.49	Moderately dry	10	1 in 10 years	Moderate drought
−1.5 to −1.99	Severely dry	5	1 in 20 years	Severe drought
≤−2.0 SPI	Extremely dry	2.5	1 in 50 years	Extreme drought

(1) Number of drought periods in 100 years.

2.3.2. Construction of Vegetation Indices

Numerous vegetation indices have been used in recent years: to estimate the leaf area index (LAI), percentage ground cover, plant height, biomass, canopy diversity, and other parameters. Most formulae (or equations) are based on ratios or linear combinations and many show differences in the values for measuring healthy vegetation and coverage [124–128]. Based on this knowledge of the different indices and their applications in the field of remote sensing, it was decided to take make complementary use of the NDVI, NDWI, and EVI: the NDVI for the normalized analysis of the vegetation vigor in order to differentiate vegetation from other types of ground cover and to determine its general condition; the NDWI to observe the amount of water in the vegetation and the level of soil moisture saturation; and the EVI to differentiate the crop vitality and water stress through the amount of chlorophyll from the vegetation covers.

Starting with the NDVI (Normalized Difference Vegetation Index), as is known, it is based on the contrast between the maximum absorption in the red band due to chlorophyll pigments and the maximum reflection in the infrared band caused by the leaf cellular structure. The NDVI is directly related to the photosynthetic capacity and, therefore, to the energy absorbed by plants. It is calculated from individual red and near-infrared measurements. In fact, the first use [129] of this vegetation index was simply the ratio of the NIR (near-infrared reflectance) and red (visible red band), although this should not be called a vegetation index. As the NDVI (Normalized Difference Vegetation Index) was first described in 1973 [130], it has the advantage of only varying from −1 to +1. This is the one used for the advantage of being able to point out small differences in the image. A great variety of NDVI modifications exist and are described by the numerous authors [131–135]. These indices are of the general form for the MODIS data:

$$\text{NDVI} = (\text{NIR} - \text{Red}) / (\text{NIR} + \text{Red}) \quad (1)$$

where R_x is the reflectance at the given wavelength (nm). The NIR in the MODIS is the reflectance or radiance in a near-infrared channel (B2), wavelength 841–876 nm. RED (B1), wavelength 620–670 nm.

The combination of its normalized difference formulation and the use of the higher absorption and reflectance regions of chlorophyll make it robust over a wide range of conditions. Despite its intensive use, the NDVI saturates in cases of a dense and multi-layered canopy and shows a non-linear relationship with biophysical parameters such as green LAI. This affects the correlation of the parameters of the NDVI with the LAI (Leaf Area Index). To correct this, different authors have improved indices like the Renormalized Difference Vegetation Index (RDVI) or developed the Modified Simple Ratio (MSR) [136], in order to linearize their relationships with the biophysical vegetation parameters of boreal forests. The RDVI (Equation (2)) was proposed to combine the advantages of the

Difference Vegetation Index ($DVI = NIR - Red$) and the NDVI for low and high LAI values, respectively. This index has been adapted of the general form:

$$RDVI = (NIR - Red) / \sqrt{(NIR + Red)} \quad (2)$$

To complement the information obtained with the NDVI, the NDWI (Normalized Difference Water Index) is used, as it refers to an index derived for remote sensing related to liquid water. It has been used by numerous authors in different circumstances [137,138] and it is used in this study to monitor changes in the leaf water content, using near-infrared reflectance (NIR) and shortwave infrared (SWIR) [139]. The NIR band collects the bright reflectance of the internal structure of the leaf and the dry matter content of the sheet and the SWIR is sensitive to the water content of the vegetation canopy and the mesophyll structure of leaves. The NDWI it is a good indicator of deforestation and compensates for the abrupt drop in the values of the NDVI when it saturates [140–142]. Therefore, this index is a useful indicator of the water status of trees when it comes to withstanding drought periods. The combination of the NIR with the SWIR eliminates the variations induced by the internal leaf structure and leaf dry matter content, which improves the accuracy in assessing whether the recovery of the crop moisture status has begun. The value of this index varies from -1 to 1 . These indices are of the general form (Equation (3)):

$$NDWI = (NIR - SWIR) / (NIR + SWIR) \quad (3)$$

where in the MODIS, the NIR is B2: 841–876 nm and the SWIR is the reflectance or radiance in a shortwave infrared wavelength channel, B6: 1628–1652 nm.

As is known, each vegetation index has limitations. In the case of the NDVI, it has been found that it is sensitive to the effects of the soil and the atmosphere; it is therefore advisable to apply other additional indices for a more precise analysis of the vegetation. To that end, we have applied an Enhanced Vegetation Index (EVI), which is like the Normalized Difference Vegetation Index (NDVI) and can be used to quantify the vegetation greenness [143–145]. However, the EVI corrects for some atmospheric conditions and canopy background noise and is more sensitive in areas with a dense vegetation. To do this, using this index, the difference in the radiance between the blue and red bands is calculated [146,147]. These indices are of the general form (Equation (4)):

$$EVI = G \times \frac{NIR - RED}{NIR + C1 \times RED - C2 \times BLUE + L} \quad (4)$$

where the NIR is B2: 841–876 nm, RED is B1: 620–670 nm, and BLUE is B3: 459–479 nm. L is a canopy background adjustment that considers the differential radiant transfer of near infrared and red through the canopy, G is a gain factor, and C1 and C2 are the aerosol resistance coefficients, which use the blue band to correct the influence of the aerosol on the red band. The coefficients adopted in the EVI algorithm are $L = 1$, $C1 = 6$, $C2 = 7.5$, and $G = 2.5$ [148].

The values of each of the applied indices show the particularities of each of the areas analyzed, but at the same time, they show the climatic characteristics they receive from their geographical location, although at the same latitude, separated longitudinally from west to east. The results of the application of the indices can be seen in Table 7 and Figure 7. The linear sum of the values of each of the indices has been made and their average value was calculated.

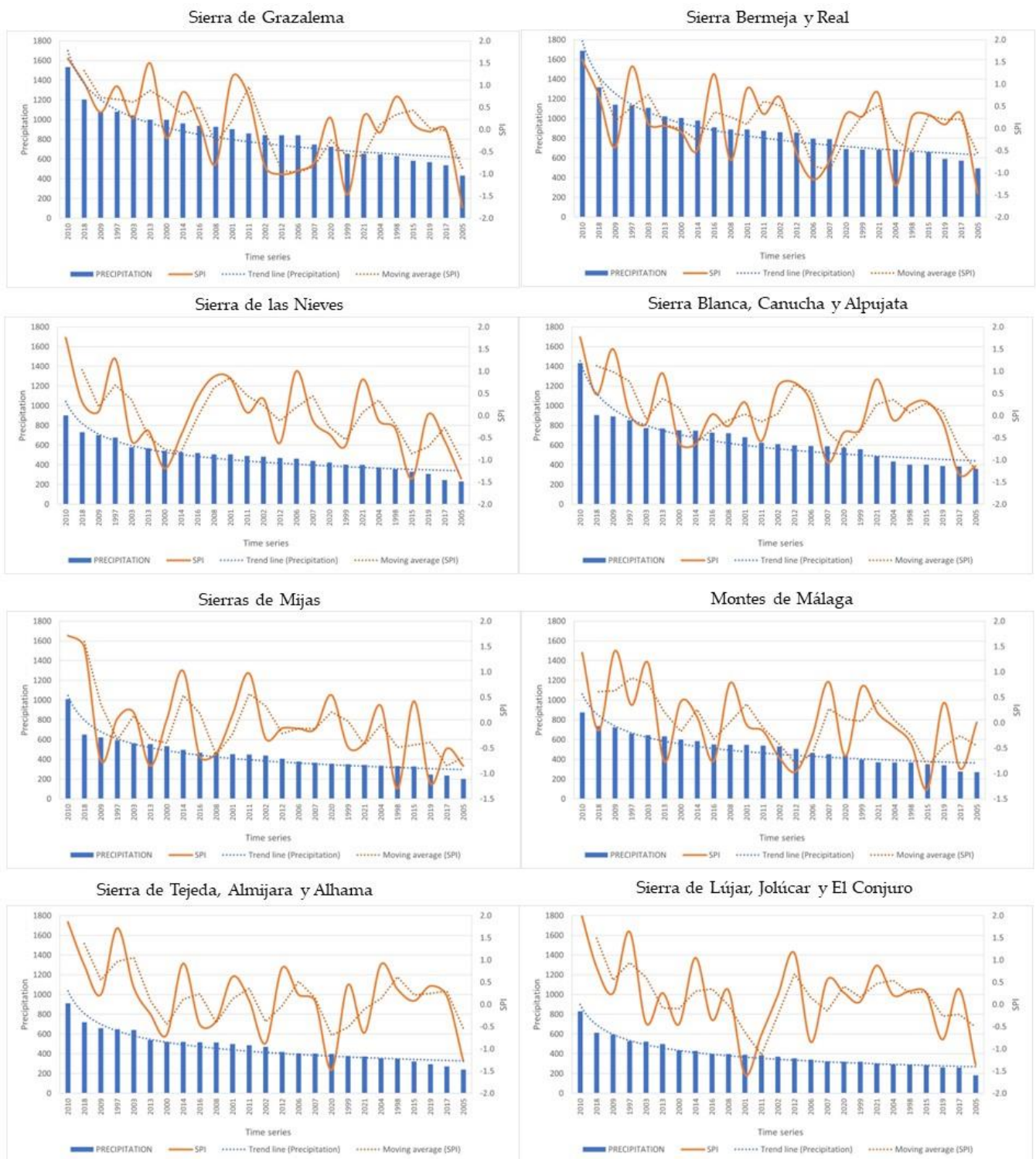


Figure 6. Cont.

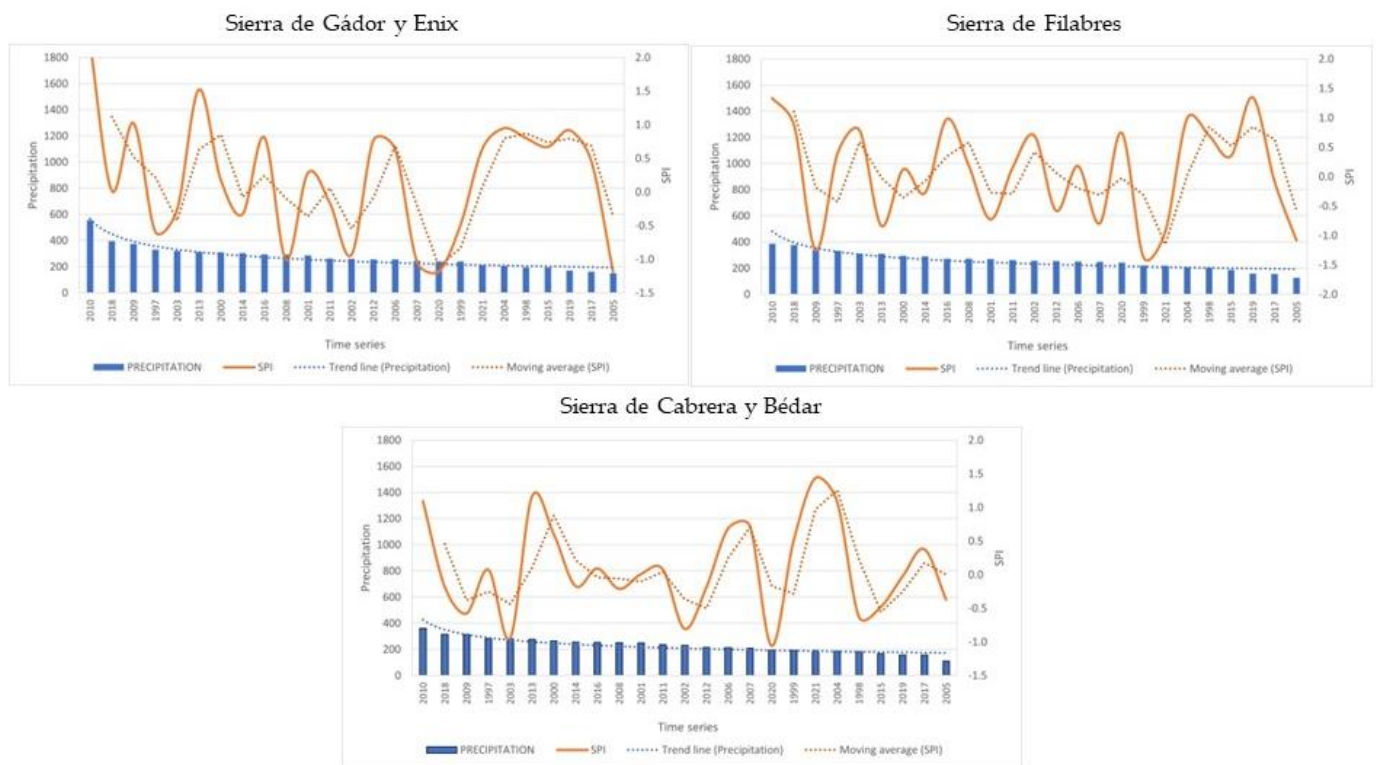


Figure 6. Annual distribution of Standardized Precipitation Index (SPI) and annual precipitation. Sorted according to defined time series, see the reference in Table 5. Clarification of the legend. The years of the time series, for comparison, are ordered on all graphs with the same sequence of years: from very wet to very dry. Own elaboration based on data of the portal <https://monitordesequia.csic.es/> (accessed on 21 December 2022) for the SPI and Automatic Hydrological Information System (SAIH) Hidrosur, Autonomous Community of Andalusia (Spain) for precipitation data <http://www.redhidrosurmedioambiente.es/saih/> (accessed on 21 December 2022).

Table 7. Average values of the vegetation indices applied (NDVI, NDWI, and EVI) for the assessment of the state of vegetation covers.

Natural Areas	Too Bad	Not Good	Acceptable	Good	Very Good
Sierra de Grazalema (SG)	−0.148–0.166	0.167–0.315	0.316–0.396	0.397–0.474	0.475–0.645
Sierras Bermeja and Real (SBR)	0.129–0.308	0.309–0.393	0.394–0.454	0.455–0.514	0.515–0.643
Sierra de las Nieves (SN)	0.118–0.234	0.235–0.309	0.310–0.384	0.385–0.459	0.460–0.577
Sierra Blanca, Canucha, and Alpujata (SBCA)	0.177–0.281	0.282–0.345	0.346–0.396	0.397–0.455	0.456–0.575
Sierra de Mijas (SM)	0.089–0.211	0.212–0.279	0.280–0.350	0.351–0.417	0.418–0.515
Montes de Málaga (MM)	0.272–0.344	0.345–0.384	0.385–0.415	0.416–0.442	0.443–0.505
Sierras de Tejeda, Almijara, and Alhama (STAA)	0.036–0.215	0.216–0.288	0.289–0.347	0.348–0.416	0.417–0.554
Sierra de Lújar, Jolúcar, and El Conjuero (SLJC)	0.139–0.235	0.236–0.280	0.281–0.323	0.324–0.372	0.373–0.475
Sierra de Gádor and Enix (SGE)	−0.067–0.148	0.149–0.195	0.196–0.242	0.243–0.295	0.296–0.413
Sierra de Filabres (SF)	0.087–0.213	0.214–0.259	0.260–0.308	0.309–0.370	0.371–0.504
Sierra de Cabrera and Bédar (SCB)	−0.010–0.172	0.173–0.211	0.212–0.252	0.253–0.299	0.300–0.405

Own elaboration based on MODIS Land Products: Land Processes DAAC at the U. S. Geological Survey EROS Data Center (EDC). <https://lpdaac.usgs.gov/> (accessed on 19 September 2022).

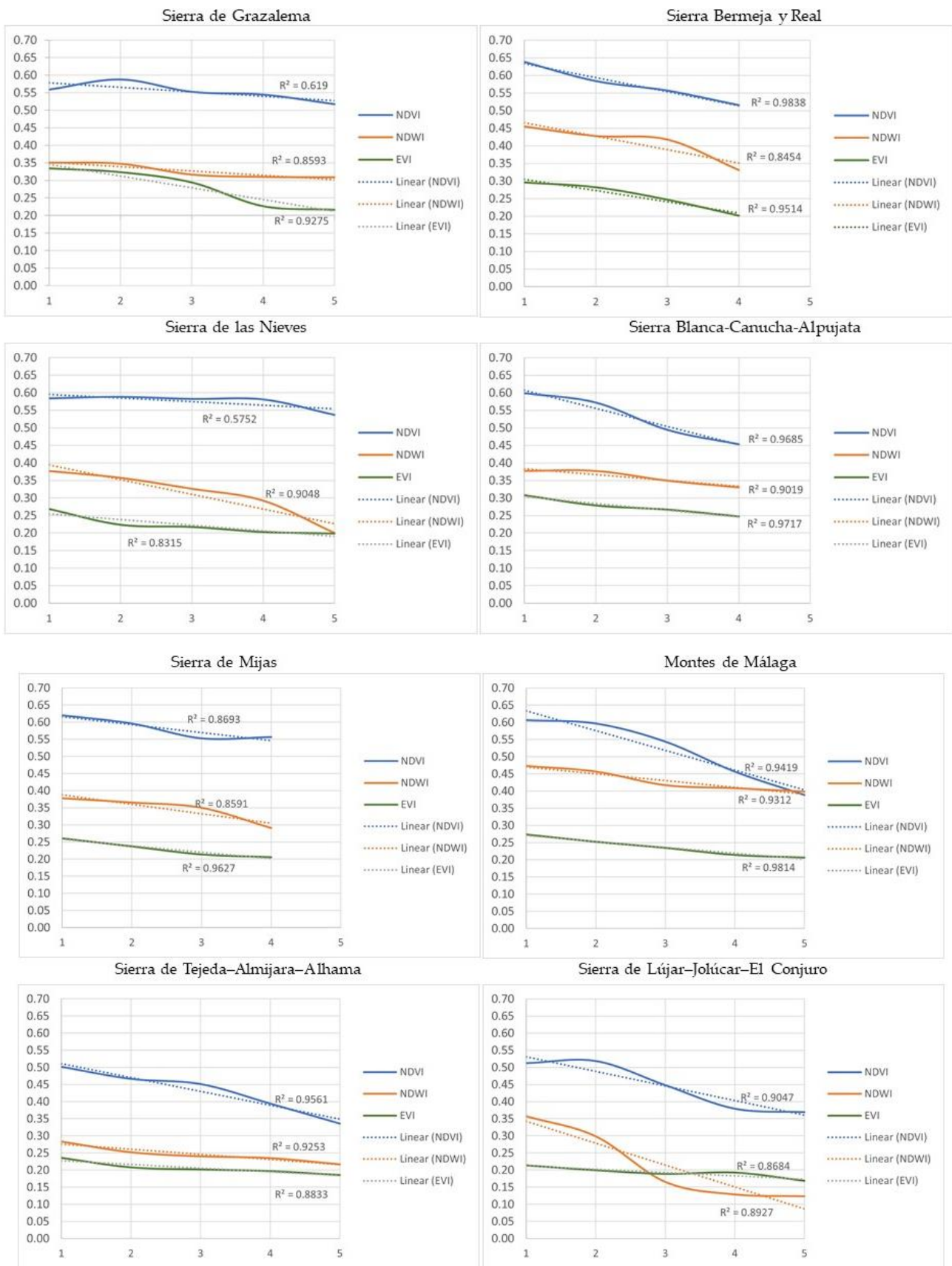


Figure 7. Cont.

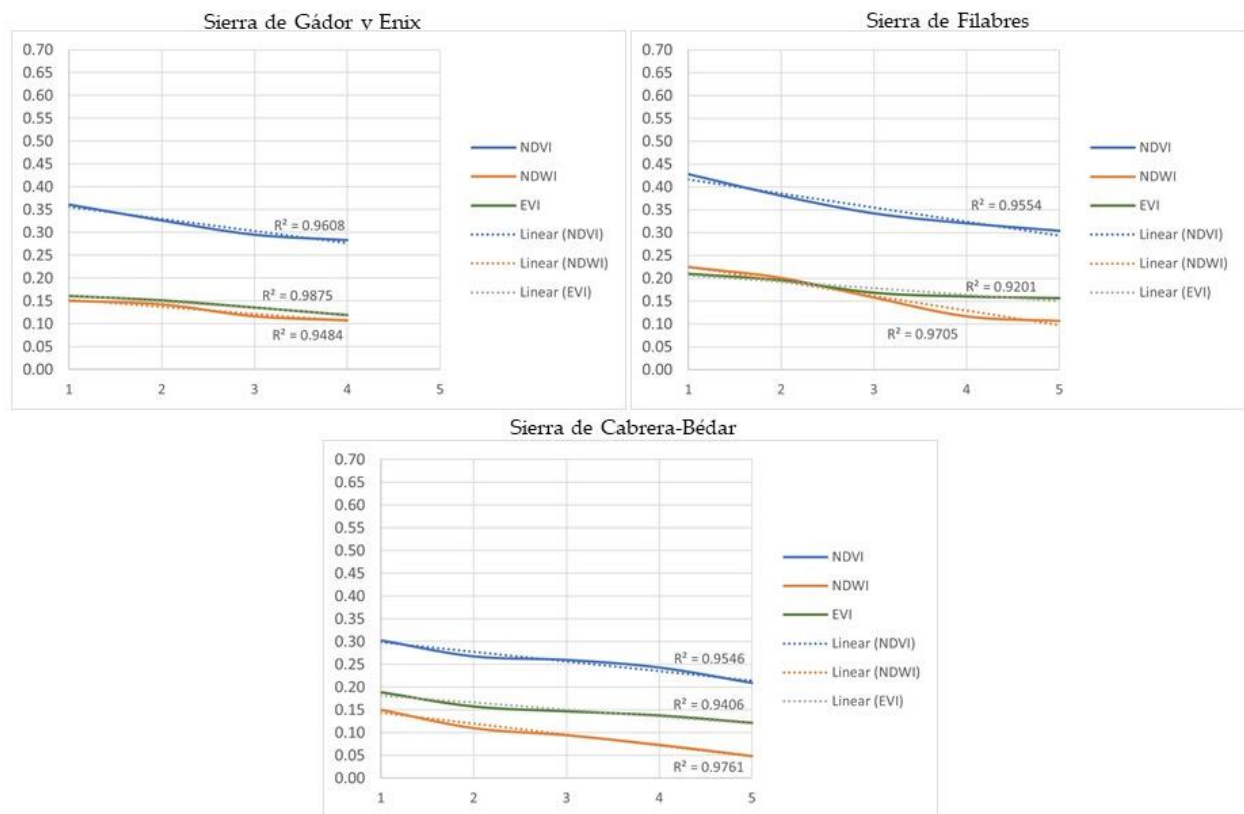


Figure 7. Average values of vegetation indices (NDVI, NDWI, and EVI) in relation to time series (1997–2021). Legend. The numeric values of the horizontal axis show the time series: 1, very wet; 2, wet; 3, mean (years around the average); 4, dry and 5, very dry. When series 5 does not appear, very dry, it means that years with that volume of precipitation have not been counted. The numeric values on the vertical axis of the chart show the values that the indices acquire. Own elaboration based on MODIS Land Products: Land Processes DAAC at the U. S. Geological Survey EROS Data Center (EDC). <https://lpdaac.usgs.gov/> (accessed on 19 September 2022).

2.3.3. Analysis of Land Use Change

Of the many technological and conceptual approaches to spatial data analysis, geographic information systems (GIS) have been widely used as a powerful tool to provide reliable information in their application to land-use change analysis [149–152]. Once this point has been reached, this methodology addresses the analysis of the land use change patterns, focusing on changes in vegetation cover and its spatial distribution. We are based on the change detection methodology developed by Pontius et al. [153,154] that has been used by numerous authors for the quantitative analysis of land use dynamics [155,156].

The analysis process begins with the establishment of the temporal criterion of the analysis, which starts in 1991 and ends in 2021. By having the land use information layers for these periods, we proceed directly to perform the analysis that starts from the overlapping of the land use layers for the established dates. The results of the operation are transferred to the transition matrix for the analyzed period. The transition matrix, or cross-tabulation matrix, is organized into rows and columns and is nourished by the information generated in the computation of the land-use layers of the given dates. The matrix arranges the classes of time cut 1 (P_i+): 1991 in the rows, and in the columns, the same classes in the temporal cut 2 (P_+): 2021. The data in these matrices acquire the following arrangement: the diagonal of the matrix is quantified by the classes of uses of the surfaces which have remained stable between the two temporal cuts, which will receive the denomination of persistence's (P_{jj}), showing each class of use that persists in class j . While outside the diagonal are the surfaces of those same classes that present transitions to other

classes of uses on the reference dates and that will receive the denomination of transitions (P_{ij}), showing the surfaces that have undergone a transition from class i to class j , that is, from one class of use to another. Such transitions can be of two types: loss (DECREASE) and gain (INCREASE). Transitions can be multiple and depend on the number of classes you have started. This is related to the levels of disaggregation of the data model that was established at the time of analysis. As mentioned, the transitions can be of two types: loss and gain. The losses expressed as L_{ij} contain the surface values of each class i that experience net losses in the period studied: 1991–2020, being its notation: $L_{ij} = P_{i+} - P_{jj}$. On the other hand, the gains expressed as G_{ij} include the values of the surfaces that experience net gains in class j in the same periods; its notation is: $G_{ij} = P_{+j} - P_{jj}$. Other calculations have been added to this process. One of total change, which should be understood as the transitions of coverage in the analyzed period. For its calculation, the notation was used: $CT = L_{ij} + G_{ij}$. Another, the net change, shows that the difference between the total values of each class for the time moments, T1: 1991 and T2: 2020; therefore, by means of the net change, the surfaces of each class that have undergone changes are quantified. The notation for the calculation of the net change was as follows: $D_j = P_{+j} - P_{j+}$. The calculation of the exchange data must show the transitions of each coverage class; especially, it makes sense to show if the changes in a class are constant and are related more to the changes in the location of a class of use in the analyzed period than to transitions of that same use, at which time its quantity would remain more or less constant if it were compared temporarily. An example of this would be that there was the appearance of a forest in a space where there was another kind of similar cover. The equation for its computation was as follows: $S_j = 2 \times \text{MIN}(P_{j+} - P_{jj}, P_{+j} - P_{jj})$.

After this process, the maps of changes have been generated, which will be valued in their state later, correlating the results with the vegetation indices which were used.

3. Results

In this section, we will analyze the results obtained from interrelating the three variables that we have applied in this work: the climatic series (precipitation and SPI), vegetation indices (NDVI, NDWI, and EVI), and land use changes. We had started from the hypothesis that the evolution of rainfall has been producing a deterioration in the vegetation covers in the biogeographic areas where natural areas are located. The study started in 1997 and ended in 2021, although the source of the data on vegetation cover dates back to 1991.

The temporal evolution of the annual precipitation was obtained for the 25-year study period. The mean annual precipitation has been observed in Table 4. The moving averages and autocorrelation treatments allowed for identifying a different cyclicity in the years 1997, 2010, which were especially wet, and 2018, highlighting these years in all the natural areas analyzed. Additionally, on the contrary, 2005 was a very dry year, with values 40% below being the average in the rainiest natural areas: Sierra de Grazalema and Sierra Bermeja and Real. Additionally, the areas with especially low rainfall in natural areas with lower precipitation values were Sierras de Lújar, Jolúcar and El Conjuero, Sierra de Gádor and Enix, Sierra de Filabres, Sierra de Cabrera, and Bédar, where records that year did not reach 200 L per m².

Regarding the SPI, Vélez-Nicolás et al. [106] have detected 26 events of drought during the 108-year period that these authors have analyzed: 1910–1911 and 2017–2018. Twelve of these events were severe ($SPI < -1.5$) and six were extreme ($SPI < -2.0$), with return periods of 9 and 18 years, respectively, for an area of study close to ours, the Strait of Gibraltar. The longest and most intensive droughts occurred during 1999–2000, 2005–2008, and 2019–2021, coinciding with some of the driest periods that have affected the European continent and the Mediterranean basin [157–159]. In Table 8, we have quantified the number of times in months and years that the different values of the SPI and precipitation have occurred during the analyzed period.

Table 8. Frequency of SPI values and annual precipitation.

Natural Areas	SG	SBR	SN	SBCA	SM	MM	STAA	SLJC	SGE	SF	SCB
SPI (1) Number of months											
Extremely wet	1	1	2	2	2	1	2	11	11	0	0
Very wet	23	19	11	13	14	9	22	18	15	15	8
Moderately wet	30	25	31	24	21	33	27	25	24	31	43
Normal wet	120	127	95	109	92	106	129	132	118	121	107
Normal dry	88	99	125	118	129	116	92	87	99	91	112
Moderately dry	19	10	15	24	32	28	15	12	22	24	28
Severely dry	13	19	21	10	10	7	10	11	11	16	2
Extremely dry	6	0	0	0	0	0	3	4	0	2	0
TOTAL, MONTHS	300	300	300	300	300	300	300	300	300	300	300
Precipitation (2) Number of years											
Very wet	1	2	2	1	1	1	2	2	1	2	1
Wet	6	4	4	5	6	6	3	4	4	6	6
Mean	9	10	11	12	9	10	12	9	13	9	9
Dry	8	9	6	7	9	6	7	9	7	5	8
Very Dry	1	0	2	0	0	2	1	1	0	3	1
TOTAL, YEARS	25	25	25	25	25	25	25	25	25	25	25

(1) The values for the evaluation of the SPI can be found in Table 6. (2) The assessment of each time series is specific to each natural area and can be consulted in Table 4. Own elaboration based on data of the portal <https://monitordesequia.csic.es/> (accessed on 21 December 2022) for the SPI and Automatic Hydrological Information System (SAIH) Hidrosur, Autonomous Community of Andalusia (Spain) for precipitation data (<http://www.redhidrosurmedioambiente.es/saih>) (accessed on 21 December 2022).

However, we have been able to verify that the annual distribution of rainfall is a pattern that is typical of Mediterranean semi-arid climates, so it is not possible to affirm categorically that we are in a scenario that could be decisive for the deterioration of vegetation covers in particular and these ecosystems in general. At least, because of this cause, it has been possible to observe that a pattern of decrease in the volume of precipitation, characterized by an increasingly irregular distribution of precipitation, is currently normalizing. Despite this, the vegetation covers have been withstanding these conditions. It is precisely the quantification of the changes produced in them that we will focus on in this section of results. In Figures 8–10, it is possible to observe the dynamics of changes that have occurred in the last 30 years. An analysis of these changes has been carried out with the intention of assessing the current state of the vegetation covers. The selected natural areas have maintained a large part of the vegetation covers that characterize them. However, there has been a dynamic of changes that have given rise to the current roof surfaces.

In Tables 9 and 10 below we can see what this dynamic of changes has been and its quantification.

At this point we have been able to observe that the surfaces of vegetation covers the forest and areas of the shrub and herbaceous vegetation which have remained in a large proportion. These represent the following proportions with respect to the total of each natural area: Sierra de Grazalema, 84.34% (44,736.94 has of 53,041.19 has); Sierra Bermeja y Real, 93.26% (26979.90 has of 28,928.70 has); Sierra de las Nieves, 97.33 % (17,902.97 has of 18,394.30 has); Sierra Blanca, Canucha, and Alpujata, 91.94% (11,200.55 has of 12,182.06 has); Sierra de Mijas, 84.99% (6633.10 has of 7804.46 has); Montes de Málaga, 92.94% (4643.15 has of 4995.60 has); Sierra de Tejeda, Almirajara, and Alhama, 97.16% (38,940.25 has of 40,078.15 has); Sierra de Lújar, Jolúcar, and El Conjuero, 87.24% (11,088.71 has of 12,709.90 has); Sierra de Gádor and Enix, 96.29% (48,444.39 has of 50,312.93 has); Sierra de Filabres, 88.85% (63,674.15 has of 71,665.37 has); and Sierra de Cabrera y Bédar, 76.91% (25,919.70 has of 33,703.49 has). For the total area of study, this proportion amounts to 89.92% (300,163.80 has of 333,816.15 has). These figures can be seen in Figure 11.

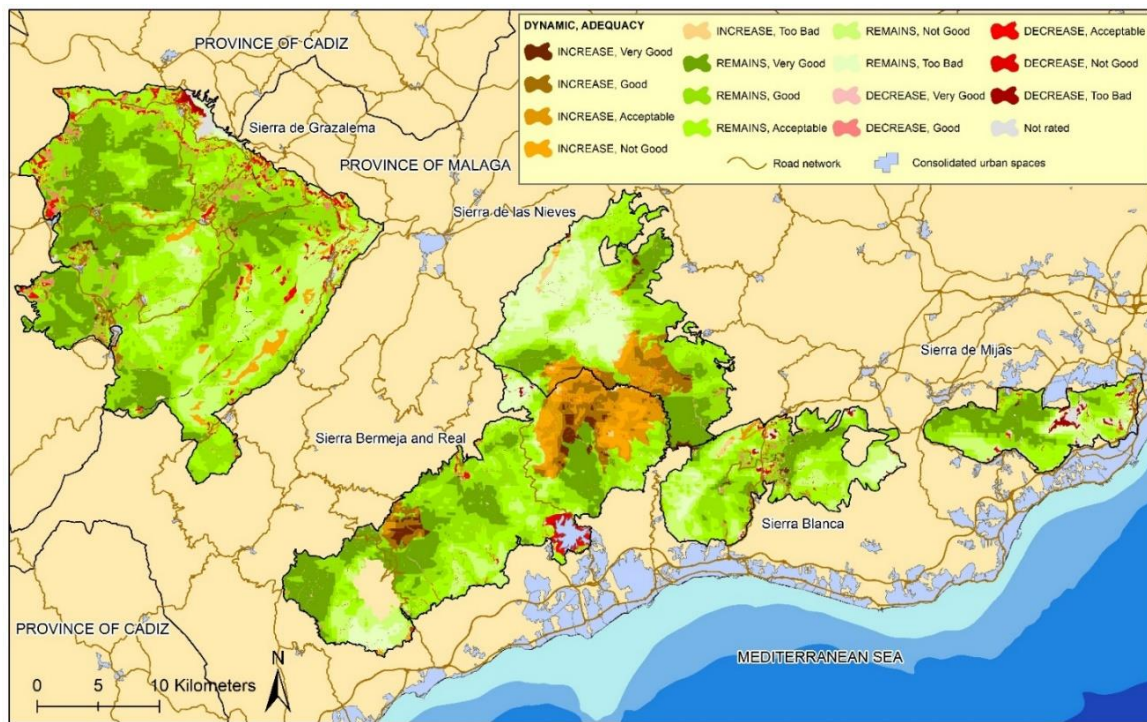


Figure 8. Dynamics of changes in vegetation cover (1991–2021). Natural areas to the west of the study area. Province of Cadiz and Malaga. Own elaboration based on data of Cartography of the Uses and Vegetation Covers of the soil of Andalusia (1991) and the Geographical Information System for the Identification of Agricultural Land Parcels (SIGPAC) (2021).

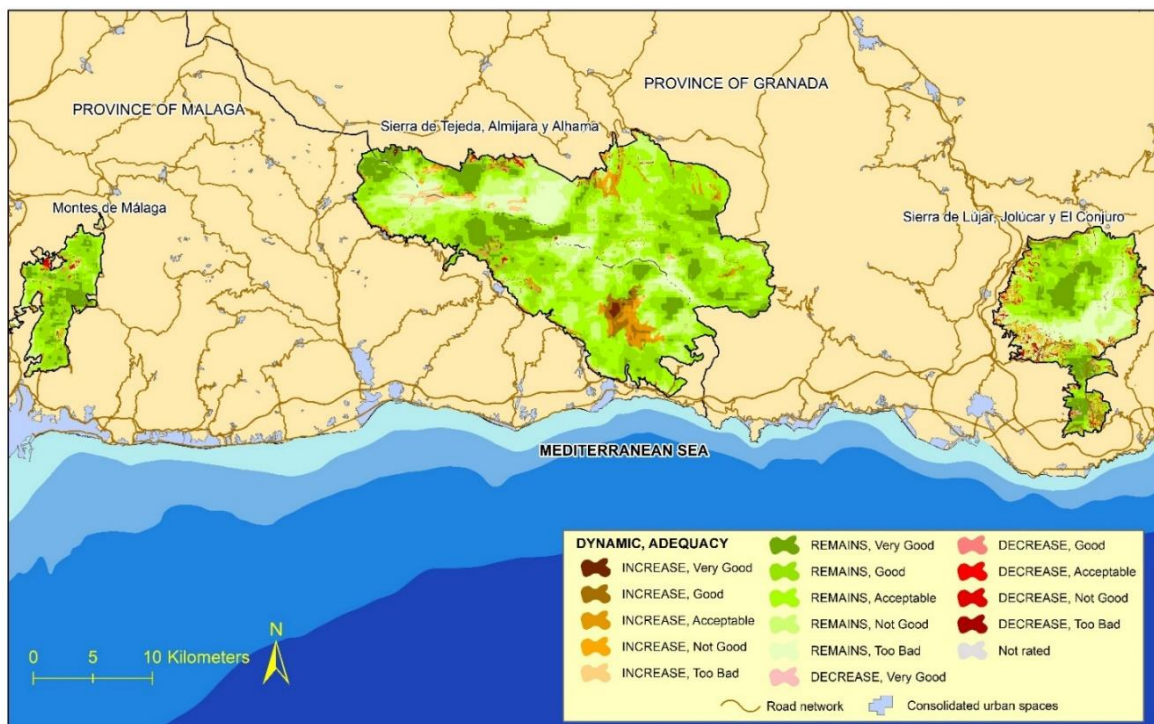


Figure 9. Dynamics of changes in vegetation cover (1991–2021). Natural areas in the middle of the study area. Province of Malaga and Granada. Own elaboration based on data of Cartography of the Uses and Vegetation Covers of the soil of Andalusia (1991) and the Geographical Information System for the Identification of Agricultural Land Parcels (SIGPAC) (2021).

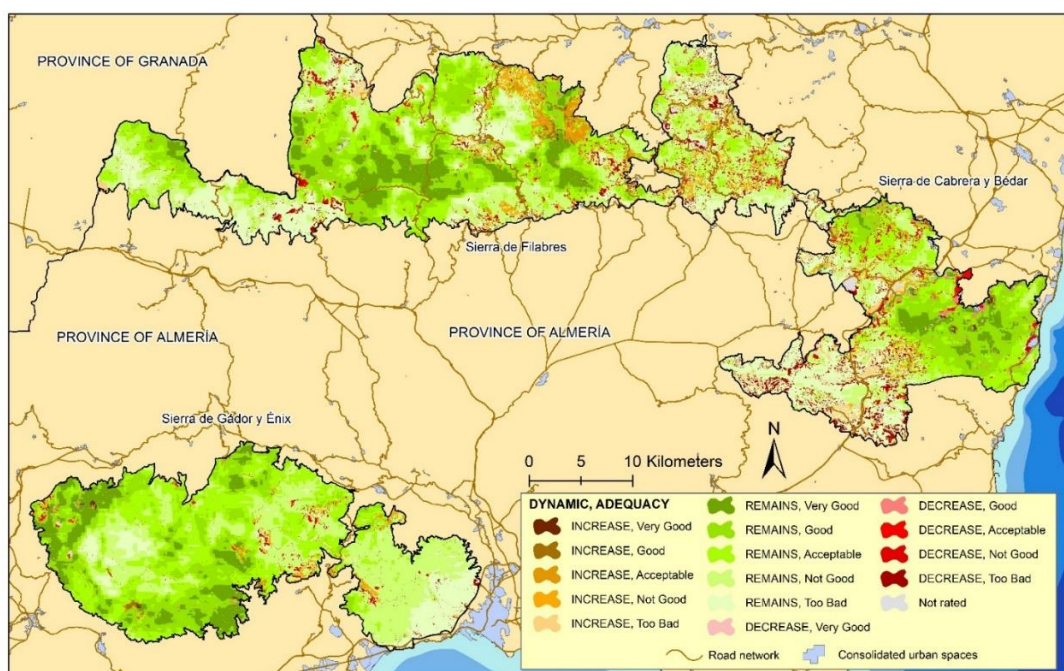


Figure 10. Dynamics of changes in vegetation cover (1991–2021). Natural areas to the east of the study area. Province of Granada and Almería. Own elaboration based on data of Cartography of the Uses and Vegetation Covers of the soil of Andalusia (1991) and the Geographical Information System for the Identification of Agricultural Land Parcels (SIGPAC) (2021).

Table 9. Dynamics of change (1991–2021). Area in hectares.

		Natural Areas											
		Dynamic	SG	SBR	SN	SBCA	SM	MM	STAA	SLJC	SGE	SF	SCB
INCREASE	CA–ASHV	972	87	66	194	56	89	416	781	583	3250	2097	
	CA–FOR	660	70	186	179	21	277	487	62	258	1226	74	
	OANOV–ASHV	756	2940	1053	167	0	0	1774	0	81	7	147	
	OANOV–FOR	256	3059	1736	0	11	0	399	0	17	16	0	
	SUBTOTAL	2643	6156	3041	540	88	367	3076	843	939	4498	2317	
REMAINS	ART	1	0	0	0	0	0	0	4	0	0	34	
	ASHV	8005	4683	3794	4044	1454	50	11,577	6090	26,491	19,216	22,125	
	FOR–ASHV	5006	2922	1707	604	299	105	3381	967	1414	3400	98	
	OAV–ASHV	936	2534	1184	1864	375	43	3095	957	2806	4007	86	
	CROPS	3275	74	17	257	85	62	188	615	237	2294	2203	
	ASVH–FOR	3071	2270	1530	734	588	134	6539	1162	10,346	7348	935	
	FOR	23,849	7136	4808	1791	3013	3433	5564	761	2325	15,819	211	
	OAV–FOR	1226	1278	1838	1624	818	510	5710	309	4123	9385	147	
	WET	782	463	172	67	81	61	287	75	313	383	397	
SUBTOTAL	46,151	21,360	15,051	10,984	6712	4400	36,340	10,940	48,056	61,853	26,236		
DECREASE	ASHV–CA	1068	40	22	105	27	44	117	492	564	2627	2906	
	FOR–CA	882	131	14	90	23	48	76	45	45	417	2	
	OANOV–CA	31	12	5	3	0	0	2	0	0	0	9	
	OAV–CA	314	10	17	22	17	22	29	15	60	460	7	
	ASHV–AA	448	177	38	76	172	7	140	190	434	628	1257	
	FOR–AA	486	831	120	109	145	74	70	46	51	297	15	
	OANOV–AA	15	47	45	2	0	0	11	0	1	1	62	
	OAV–AA	53	85	21	64	103	14	96	6	66	194	2	
SUBTOTAL	3296	1333	282	470	486	209	542	795	1220	4624	4261		
OT	ART	951	79	20	187	519	20	121	132	98	689	889	
	TOTAL	53,041	28,929	18,394	12,182	7804	4996	40,078	12,710	50,313	71,665	33,703	

Legend natural areas: SG: Sierra de Grazalema; SBR: Sierra Bermeja and Real; SN: Sierra de las Nieves; SBCA: Sierra Blanca, Canucha, and Alpujata; SM: Sierra de Mijas; MM: Montes de Málaga; STAA: Sierra de Tejeda, Almijara, and Alhama; SLJC: Sierra de Lújar, Jolúcar, and El Conjuero; SGE: Sierra de Gádor and Enix; SF: Sierra de los Filabres; SCB: Sierra de Cabrera and Bédar.

Table 10. Legend dynamics of changes: acronym legend.

Changes	Acronym	Dynamic
INCREASE	CA-ASHV	From cultivated areas to areas of shrub and herbaceous vegetation.
	CA-FOR	From cultivated areas to forest.
	OANOV-ASHV	From open areas no vegetation to areas of shrub and herbaceous vegetation.
	OANOV-FOR	From open areas no vegetation to forest.
REMAINS	ART	Facilities, buildings, and road network with connection to the natural areas.
	ASHV	areas of shrub and herbaceous vegetation.
	FOR-ASHV	From forest to areas of shrub and herbaceous vegetation.
	OAV-ASHV	From open areas with vegetation to areas of shrub and herbaceous vegetation.
	CROPS	Cultivated areas.
	ASHV-FOR	From areas of shrub and herbaceous vegetation to forest.
	FOR	Forest.
DECREASE	OAV-FOR	From open areas with vegetation to forest.
	WET	Wetlands, water channels, and sheets.
	ASHV-CA	From areas of shrub and herbaceous vegetation to cultivated areas.
	FOR-CA	From forest to cultivated areas.
	OANOV-CA	From open areas no vegetation to cultivated areas.
OT (OTHER)	OAV-CA	From open areas with vegetation to cultivated areas.
	ASHV-AA	From areas of shrub and herbaceous vegetation to artificial areas.
	FOR-AA	From forest to artificial areas.
	OANOV-AA	From open areas no vegetation to artificial areas.
OAV-AA	From open areas with vegetation to artificial areas.	
OT (OTHER)	ART	Other areas not included in the above: network of unpaved roads, technical buildings, urban sprawl, etc.

Own elaboration.

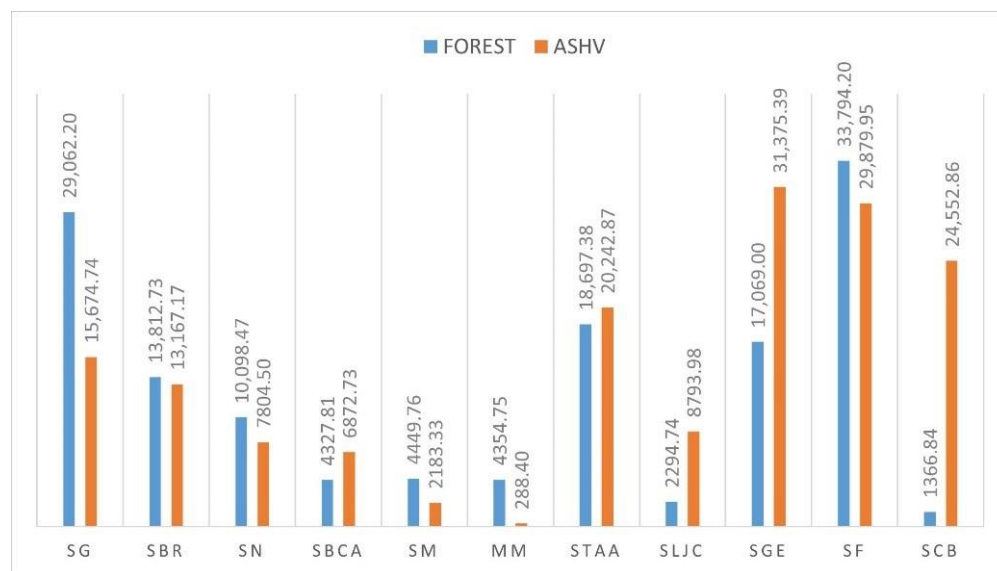


Figure 11. Current surfaces of the main vegetation cover in the natural areas in hectares (2021). Legend: SG: Sierra de Grazalema; SBR: Sierra Bermeja and Real; SN: Sierra de las Nieves; SBCA: Sierra Blanca, Canucha, and Alpujata; SM: Sierra de Mijas; MM: Montes de Málaga; STAA: Sierra de Tejada, Almijara, and Alhama; SLJC: Sierra de Lújar, Jolúcar, and El Conjuro; SGE: Sierra de Gádor y Enix; SF: Sierra de Filabres; SCB: Sierra de Cabrera y Bédar. Own elaboration based on data of Cartography of the Uses and Vegetation Covers of the soil of Andalusia (1991) and the Geographical Information System for the Identification of Agricultural Land Parcels (SIGPAC) (2021).

Although we talk about the maintenance of the vegetation covers that form the ecosystems of the natural areas studied, but these surfaces present an uneven state of

conservation, based on the analysis carried out with the application of vegetation indices, as can be seen in Table 11.

Table 11. Dynamics of change (1991–2021) and assessment of conservation status according to vegetation indices (NDVI, NDWI, and EVI) of forest areas and areas of shrub and herbaceous vegetation uses. Area in hectares.

N.A.	Dynamic (1)	Too Bad	%	Not Good	%	Acceptable	%	Good	%	Very Good	%	Total
SG	Increase	17.17	0.65	1001.53	37.89	809.60	30.63	686.99	25.99	128.10	4.85	2643.39
	Remains	97.15	0.23	6636.95	15.77	11,033.94	26.21	13,150.33	31.24	11,175.16	26.55	42,093.53
	Decrease	1.86	0.08	225.71	9.83	1143.09	49.81	864.58	37.67	59.88	2.61	2295.12
	Nat. Area	352.75	0.67	8920.01	16.82	15,361.59	28.96	15,820.08	29.83	11,635.62	21.94	53,041.16
SBR	Increase	51.33	0.83	1334.49	21.68	2440.79	39.65	1702.08	27.65	627.61	10.19	6156.29
	Remains	1624.67	7.80	3736.19	17.94	1429.29	6.86	6957.75	33.41	7075.70	33.98	20,823.60
	Decrease	5.70	2.95	8.65	4.48	71.50	37.02	57.35	29.69	49.95	25.86	193.16
	Nat. Area	1747.18	6.04	5445.88	18.83	4633.59	16.02	9091.08	31.43	8010.98	27.69	28,928.71
SN	Increase	219.24	7.21	330.45	10.87	1289.36	42.40	1052.70	34.62	149.28	4.91	3041.04
	Remains	2951.18	21.43	2348.86	17.06	2814.53	20.44	2941.51	21.36	2714.12	19.71	13,770.20
	Decrease	3.32	5.23	9.10	15.46	10.41	17.68	29.48	50.06	6.82	11.58	58.89
	Nat. Area	3206.75	17.43	3141.73	17.07	4550.67	24.74	4566.51	24.83	2928.64	15.92	18,394.30
SBCA	Increase	65.32	12.09	79.19	14.66	151.06	27.96	168.48	31.19	76.20	14.10	540.24
	Remains	700.01	6.57	2816.78	26.42	3348.58	31.41	2742.57	25.73	1052.31	9.87	10,660.24
	Decrease	3.32	1.51	27.30	12.43	50.67	23.08	104.06	47.39	34.25	15.59	219.60
	Nat. Area	827.19	6.79	3037.08	24.93	3669.55	30.12	3217.64	26.41	1243.19	10.21	12,181.99
SM	Increase	0.00	0.00	16.74	19.07	46.78	53.30	10.55	12.03	13.69	15.60	87.77
	Remains	381.10	5.82	1225.17	18.72	1655.63	25.29	1567.39	23.95	1716.10	26.22	6545.41
	Decrease	1.56	2.35	13.76	20.72	29.84	44.93	16.35	24.62	4.90	7.38	66.41
	Nat. Area	576.59	7.39	1427.04	18.28	1861.24	23.85	1647.08	21.10	1773.82	22.73	7804.62
MM	Increase	104.78	28.58	132.99	36.27	104.00	28.37	18.01	4.91	6.84	1.87	366.63
	Remains	192.09	4.49	602.25	14.08	1163.63	27.21	1622.26	37.93	696.26	16.28	4276.48
	Decrease	17.53	15.41	44.62	39.23	34.40	30.25	16.66	14.65	0.52	0.46	113.73
	Nat. Area	347.20	6.95	833.05	16.68	1364.93	27.32	1712.17	34.27	718.29	14.38	4995.49
STAA	Increase	382.02	12.42	450.48	14.65	1331.04	43.28	791.70	25.74	120.24	3.91	3075.49
	Remains	3094.98	8.63	8232.16	22.95	12,233.39	34.11	8504.62	23.71	3799.66	10.59	35,864.80
	Decrease	0.00	0.00	31.10	13.81	92.59	41.13	93.05	41.33	8.39	3.73	225.13
	Nat. Area	3497.34	8.73	8888.61	22.18	13,962.85	34.84	9629.02	24.03	3979.40	9.93	40,078.12
SLJC	Increase	72.08	8.56	359.82	42.71	251.06	29.80	146.20	17.35	13.36	1.59	842.51
	Remains	1518.70	14.82	2185.62	21.33	2480.43	24.21	2437.86	23.79	1623.60	15.85	10,246.20
	Decrease	34.57	6.26	194.04	35.12	186.31	33.72	114.13	20.65	23.53	4.26	552.57
	Nat. Area	1711.76	13.47	3108.54	24.46	3200.69	25.18	2838.33	22.33	1718.68	13.52	12,709.89
SGE	Increase	48.47	5.16	346.42	36.88	345.38	36.77	143.11	15.24	55.92	5.95	939.31
	Remains	4435.14	9.34	15,762.40	33.18	13,449.83	28.31	8972.38	18.89	4885.14	10.28	47,504.90
	Decrease	39.24	5.86	306.86	45.86	198.10	29.60	91.66	13.70	33.30	4.98	669.17
	Nat. Area	4716.91	9.38	16,751.90	33.30	14,282.58	28.39	9395.61	18.67	5067.96	10.07	50,312.70
SF	Increase	853.89	18.98	1865.58	41.47	1367.49	30.40	389.17	8.65	22.14	0.49	4498.27
	Remains	11,936.51	20.17	18,552.99	31.35	12,732.91	21.52	10,573.14	17.87	5380.20	9.09	59,175.75
	Decrease	1047.73	29.90	1702.26	48.58	615.81	17.58	118.86	3.39	19.18	0.55	3503.84
	Nat. Area	14,787.96	20.63	23,728.85	33.11	15,503.89	21.63	11,446.50	15.97	5508.58	7.69	71,665.18
SCB	Increase	1198.41	51.71	631.68	27.26	306.74	13.24	104.24	4.50	76.35	3.29	2317.42
	Remains	5439.88	23.05	5396.03	22.86	5538.51	23.47	5571.15	23.60	1656.62	7.02	23,602.20
	Decrease	1224.05	41.85	839.77	28.71	528.51	18.07	254.27	8.69	77.96	2.67	2924.56
	Nat. Area	9390.80	27.86	7937.11	23.55	7104.35	21.08	6402.89	19.00	1979.02	5.87	33,703.22

(1) The concepts increase, remains, and decrease only include the quantification and valuation of land change in forest and areas of shrub and herbaceous vegetation uses. Other uses have not been included: artificial, crops, and wetlands, although they are in the field called natural area. Legend natural areas: SG: Sierra de Grazalema; SBR: Sierra Bermeja and Real; SN: Sierra de las Nieves; SBCA: Sierra Blanca, Canucha, and Alpujata; SM: Sierra de Mijas; MM: Montes de Málaga; STAA: Sierra de Tejada, Almijara, and Alhama; SLJC: Sierra de Lújar, Jolúcar, and El Conjuero; SGE: Sierra de Gádor and Enix; SF: Sierra de Filabres; SCB: Sierra de Cabrera and Bédar. Own elaboration based on data of Cartography of the Uses and Vegetation Covers of the soil of Andalusia (1991) and the Geographical Information System for the Identification of Agricultural Land Parcels (SIGPAC) (2021).

4. Discussion

We started from the hypothesis that the Mediterranean ecosystems of Europe and, specifically, those of southern Spain are suffering differently from the climatic conditions imposed by climate change [1,2,4]. These spaces have usually endured very variable weather situations [12–14]. One of the most determining variables is the regime of rainfall and the occurrence of droughts [8,9]. That is why we have focused on the water balance. However, this circumstance has also been conditioned because we have not been able to

configure a temperature database with a sufficient resolution and amplitude to cover a series of a minimum of 25 or 30 years, as would have been necessary to be able to use it together with the rainfall database. We are aware that the analysis of the time series can be completed with another climatic variable such as temperatures or evapotranspiration [34]. However, we consider that the results of the evaluation carried out are consistent with the observed evolution of vegetation covers during the last 30 years in the study area according to the comparison we have made with other studies such as those of Novillo et al. [160], Martínez-Fernández et al. [161], or Lasanta et al. [162].

For the study period, the distribution of the average monthly precipitation showed a marked variability during all the years of the period studied, with rainfall being concentrated in some years and having low or very low values in others, a characteristic feature of Mediterranean climates. Regarding the evolution of precipitation, the moving averages and autocorrelation treatments allowed us to identify a low cyclicity, although they did show certain zonal differences.

In the first place, the number of wet years is similar in all the natural areas (between 4 and 6 years) regardless of their geographical location, whether further west or further east of the territory of Andalusia. This has its origin in the fact that the storms follow a trajectory from west to east, entering with more active fronts from the west or southwest and sweeping the Mediterranean coast to the east, where they arrive weaker. This largely explains why the average rainfall is in the natural areas to the west between 700 and 900 mm: Sierra de Grazalema, Sierra Bermeja and Real, Sierra de las Nieves and Sierra Blanca, Canucha, and Alpujata. While to the east the records are below 400 mm: Sierra de Lújar, Jolúcar and El Conjuero, Sierra de Gádor and Enix, Sierra de los Filabres, and Sierra de Cabrera and Bédar. In between are the natural areas that receive quantities between 700 and 400 mm: Sierra de Mijas; MM: Montes de Málaga; and STAA: Sierra de Tejada, Almjara, and Alhama.

Secondly, in terms of the evolution of precipitation, we have observed that the three main series: dry periods, which we have called as the periods around the average and wet periods which alternate, following a frequency of one or two years. This situation is accompanied by a slight increase in the irregularity of rainfall and a greater frequency of extreme events: drought and heavy rainfall concentrated in certain years. We observe that periods of drought tend to be longer, something that is observed in the number of dry or very dry years, which have been 8 years or more in the 25-year period studied. Recent studies have found decreasing precipitation trends in the second half of the 20th century in the Andalusian–Mediterranean coastal area [163]. This fact has been evidenced by the information provided by the analysis of the SPI. According to the consulted works of some authors [106,157,158,163], the analysis of the SPI shows that there is a differential behavior between the natural areas further west and the one that are further east, fundamentally determined by the rainfall regime that predominates in each of these areas. These conclusions agree with the data provided by Merino et al. [164], who refer to a trend towards the appearance of the negative results of the index. Although, other studies that used fewer observatories with precipitation records and that extend until the beginning of the 20th century have not detected appreciable changes in annual precipitation [53,165]. In view of this, it can be affirmed that in the precipitation trends during the last decades for the south of the Iberian Peninsula, negative data alternate with short periods of strong positive anomalies, results that coincide with those of Peña-Gallardo et al. [166], García-Barrón et al. [167], Lana and Burgueño [4], and Sousa et al. [168], who also detected an increase in the rainfall variability in Andalusia and in the southwest region of the Iberian Peninsula, respectively, especially during the last third of the 20th century.

In another order of things, we have observed that the changes in the vegetation cover and evolution of the ecosystems have been conditioned in a large part by the different climatic stages that have occurred in the south of the Iberian Peninsula, as evidenced by Paredes et al. [169]; specifically in its Mediterranean area during the period studied according to Aguilar-Alba [170]. The beginning of the sequence shows green covers in

accordance with the characteristics of the Mediterranean climate, where it is common for wetter periods to occur with drier periods, the driest being increasingly prolonged.

According to Novillo et al. [160], a clear response of vegetation indices to the more arid conditions of this period is observed. The variability in the changes, according to the data of the surfaces and percentages corresponding to each type, suggests specific deforestation events, which are variable in each of the natural areas studied. Although these are not collected systematically and permanently, since the surfaces that have remained in the same type of cover represent a high percentage within each space, as could be seen in Table 10. On the other hand, there have been changes in land uses due to the implementation of uses that we have called artificial and that, in some cases, are a part of the infrastructure of the natural area, or in others they are not in accordance or are not related to it, although the surfaces related to these uses are really small, less than 5%, except in Sierra de Mijas, which stands at 6.65% of the surface (518.85 has).

In general, the results of the method followed suggest that climate changes, mainly those related to the water conditions, are influencing the evolution and transformation of the vegetation covers that characterize the ecosystems of each of the natural areas studied. However, these changes can be conditioned in turn by the degree of human pressure on each of them, mainly in relation to the cultivation of new areas or the abandonment of existing ones. In this sense, the most remarkable cultivated areas are within the natural areas of Sierra de Grazalema occupying an area of 5570.21 hectares (10.50% of the surface of this space), Sierra de Lújar, Jolúcar, and El Conjuero with 1167.81 hectares (9.19%), Sierra Filabres with 5798.09 hectares (8.09%), and Sierra de Cabrera and Bédar with 5127.36 hectares (15.21% of the total area). It is noteworthy that these crop areas are in a good condition in most cases. There is only an obvious risk of the deterioration of the spaces when the crops are abandoned, and in the transition stage towards the climatic vegetation, there is a deterioration of the areas they occupied. In some cases, the geoecological consequences of an agricultural abandonment are evident, in such a way that the plant colonization processes, and geomorphological processes are triggered in the abandoned agricultural space within the natural area that can cause a deterioration of the ecosystem of these areas. During the cultivation phase, the farmer has carried out a series of conditioning that, when abandoned, causes natural processes of plant recolonization and erosion with soil losses according to the evidence cultivated by Regos et al. [171] or Palombo et al. [172].

5. Conclusions

With the method provided, it will be possible to have a procedure that allows a broad and detailed knowledge of the changes in uses and roofs and their state of conservation. To contrast the results of our analysis, we propose an area of experimentation. In this area we will check the starting hypothesis and the method designed. For this, very significant spaces of the situation addressed are proposed: they will be the natural spaces of the Mediterranean biogeographical region concerning the southern provinces of Spain of Cádiz, Málaga, Granada, and Almería.

The study of the various types of sources and the methodology applied has helped us to advance in the knowledge of the evolution of human interventions in the natural areas studied. It has become clear that the use and management of green covers leaves its mark on the ecosystems of natural areas. We emphasize that it is essential to influence the differentiation between natural and anthropogenic behaviors in the changes in land use and changes in the vegetation cover. This is to avoid the possible masking of a natural climatic evolution. This involves the search for common guidelines, based on as many data as possible and the application of a coherent method, to discern whether the areas potentially little affected by human activities, such as the natural areas studied, have responded in their dynamics to one cause or another. The great variability in the anthropogenic activity in southern Spain, in response to a complex pattern of human activities, in the biogeographic spaces of severe topography and climatology, may determine the future evolution of its natural areas. It seems that the constant threat of forest fires that beset them every summer

will be a part of it. It is important to be aware that man's relationship with natural spaces during the last decades goes through his ability to modify and mask the natural evolution of these spaces and whether there is a subordination of the anthropogenic activities to changes in climate.

For all the analysis and the scientific literature consumed, we can understand that the Mediterranean character of the Andalusian climate will not change but that the tendency is that it will be accentuated both in its amplitude (the dry and warm months of the year) and in its depth (the magnitude of aridity). This aridity will extend from the driest and warmest bioclimatic units, taking the place of the cool and humid enclaves, producing a simplification of the climatic diversity of Andalusia. This will affect the natural areas to different degrees and each of them will face a process of resilience that should be monitored with methods such as the one we provide. The above statements are based on the reports that the different administrations of the Spanish State have been publishing. In this sense, the different administrations have been promoting numerous studies and reports to monitor the current and future impacts of climate change in the Spanish territory. Among them, we highlight the Evaluation Reports of the IPCC [173], the reports of the Transparency Portal of the General State Administration [174], or the reports of the Andalusian Portal of Climate Change [175]. These studies are based on the use of a historical series of precipitation and temperatures. The temperature and precipitation series of more than 2300 stations and climate models, such as CGCM2 and ECHAM4/OPYC3 for the periods of 1960–2100 and 1990–2100, respectively. Finally, periodic contributions are also being made regarding the guidelines for the management of natural areas for the maintenance of ecosystem biodiversity, such as the monograph entitled: water accounts [176].

An applied approach has been given because, in this work, it is understood that the current technological and methodological solutions must be brought closer to the managers of natural areas (local, regional, or national) to address one of the most important aspects that can hinder their conservation: the evolution of the state of the vegetation covers due to the variability in the climatic conditions. The importance of this problem increases in a real context of climate change, which will further limit the availability of water resources due to the scarcity and irregularity of rainfall. This situation can lead to the deterioration of the biodiversity of natural areas, which, at the same time, suffer the constant threat of forest fires. Added to this is the social pressure of economic agents on them, who demand a wider economic use. To face the aforementioned challenges, researchers must provide the technology and tools necessary to assess their status and thus have the updated knowledge to manage these spaces: assessing the conservation status of forest masses in a very changing context imposed by climate change we believe is a crucial aspect for the design of conservation actions.

We understand that the sustainable territorial management of natural areas cannot be carried out simply by considering them as an isolated spaces from their environment and that they must be understood in the territorial framework that hosts them.

It is clear that the ecosystems of natural areas, which have maintained their adaptation to climatic conditions, may now see their biodiversity endangered by other human-induced causes such as the abandonment of agricultural crops in their spaces, the increase in forest fires, which are caused by human action in most cases and are becoming increasingly voracious, and by the urban pressures that come from its area of influence. These are aspects that must be addressed urgently by the administrations. Additionally, for this, instruments, and methods of analysis such as the one we have proposed in this study are needed.

The areas of influence of these will play a crucial role in the future of their conservation since in these areas we find multiple activities that each day enforce a greater pressure on these spaces. Various questions arise: how can the biodiversity conditions of these spaces, protected or not, be maintained in very dynamic territories? We think that it will not be possible to preserve natural areas without regulating and ordering the uses of the areas that surround them.

Author Contributions: Conceptualization, F.B.G.-J. and S.R.-C.; methodology, F.B.G.-J.; software, P.Q.-M.; validation, F.B.G.-J., P.Q.-M., D.C.-H. and S.R.-C.; formal analysis, F.B.G.-J., P.Q.-M. and D.C.-H.; investigation, F.B.G.-J. and S.R.-C.; resources, F.B.G.-J., P.Q.-M., D.C.-H. and S.R.-C.; data curation, P.Q.-M. and D.C.-H.; writing—original draft preparation, F.B.G.-J., D.C.-H. and S.R.-C.; writing—review and editing, F.B.G.-J.; visualization, F.B.G.-J., P.Q.-M., D.C.-H. and S.R.-C.; supervision, F.B.G.-J.; project administration, F.B.G.-J.; funding acquisition, F.B.G.-J. All authors have read and agreed to the published version of the manuscript.

Funding: This research is part of the project: Effects of Land Use Changes on Eco-Geomorphological Dynamics in Mediterranean Environments, At Different Scales, In the Context of Global Change. Funding number: PID2019-104046RB-I00. Was funded by the MINECO (Ministry of Economic Affairs and Digital Transformation) and 2019 Call for “I + D + I Projects” within the Framework of State Programs for the Generation of Knowledge and Scientific and Technological Strengthening of the I + D + I System and I + D + I oriented to the Challenges of Society. And partial funding for open access charge: University of Málaga and Consortium of University Libraries of Andalusia (CBUA acronym in Spain).

Institutional Review Board Statement: Not applicable.

Informed Consent Statement: Not applicable.

Data Availability Statement: Not applicable.

Acknowledgments: Thanks to José Damián Ruiz Sinoga of the Department of Geography of the University of Malaga.

Conflicts of Interest: The authors declare no conflict of interest.

References

- Morales, J.; García-Barrón, L.; Aguilar-Alba, M.; Sousa, A. Hazard Characterization of the Annual Maximum Daily Precipitation in the Southwestern Iberian Peninsula (1851–2021). *Water* **2022**, *14*, 1504. [\[CrossRef\]](#)
- Rodrigo, F.S.; Trigo, R.M. Trends in Daily Rainfall in the Peninsular Spain from 1951 to 2002. *Int. J. Climatol.* **2007**, *27*, 513–529. [\[CrossRef\]](#)
- Serrano, A.; Mateos, V.L.; García, J.A. Trend Analysis of Monthly Precipitation over the Iberian Peninsula for the Period 1921–1995. *Phys. Chem. Earth Part B Hydrol. Ocean. Atmos.* **1999**, *24*, 85–90. [\[CrossRef\]](#)
- Lana, X.; Burgueño, A. Some Statistical Characteristics of Monthly and Annual Pluviometric Irregularity for the Spanish Mediterranean Coast. *Theor. Appl. Climatol.* **2000**, *65*, 79–97. [\[CrossRef\]](#)
- Serrano, A.; García, A.J.; Mateos, V.L.; Cancillo, M.L.; Garrido, J. Monthly Modes of Variation of Precipitation Over the Iberian Peninsula. *J. Clim.* **1999**, *12*, 2894–2919. [\[CrossRef\]](#)
- González-Hidalgo, J.C.; Peña-Angulo, D.; Brunetti, M.; Cortesi, C. Recent Trend in Temperature Evolution in Spanish Mainland (1951–2010): From Warming to Hiatus. *Int. J. Climatol.* **2016**, *36*, 2405–2416. [\[CrossRef\]](#)
- Brunet, M.; Jones, P.D.; Sigró, J.; Saladié, O.; Aguilar, E.; Moberg, A.; Della-Marta, P.; Lister, D.; Walther, A.; López, D. Temporal and Spatial Temperature Variability and Change over Spain during 1850–2005. *J. Geophys. Res.* **2007**, *112*, D12117. [\[CrossRef\]](#)
- Insua-Costa, D.; Senande-Rivera, M.; Llasat, M.C.; Minguez-Macho, G. A global perspective on western Mediterranean precipitation extremes. *Npj Clim. Atmos. Sci.* **2022**, *5*, 9. [\[CrossRef\]](#)
- Llasat, M.C.; Del Moral, A.; Cortés, M.; Rigo, T. Convective precipitation trends in the Spanish Mediterranean región. *Atmos. Res.* **2021**, *257*, 105581. [\[CrossRef\]](#)
- Halifa-Marín, A.; Lorente-Plazas, R.; Pravia-Sarabia, E.; Montávez, J.P.; Jiménez-Guerrero, P. Atlantic and Mediterranean influence promoting an abrupt change in winter precipitation over the southern Iberian Peninsula. *Atmos. Res.* **2021**, *253*, 105485. [\[CrossRef\]](#)
- Esbri, L.; Rigo, T.; Llasat, M.C.; Aznar, B. Identifying Storm Hotspots and the Most Unsettled Areas in Barcelona by Analysing Significant Rainfall Episodes from 2013 to 2018. *Water* **2021**, *13*, 1730. [\[CrossRef\]](#)
- Hochman, A.; Marra, F.; Messori, G.; Pinto, J.G.; Raveh-Rubin, S.H.; Yosef, Y.; Zittis, G. Extreme weather and societal impacts in the eastern Mediterranean. *Earth Syst. Dynam.* **2022**, *13*, 749–777. [\[CrossRef\]](#)
- Kouroutzoglou, J.; Flocas, H.A.; Keay, K.; Hatzaki, M. Climatological aspects of explosive cyclones in the Mediterranean. *Int. J. Climatol.* **2011**, *31*, 1785–1802. [\[CrossRef\]](#)
- Nissen, K.M.; Leckebusch, G.C.; Pinto, J.G.; Renggli, D.; Ulbrich, S.; Ulbrich, U. Cyclones causing wind storms in the Mediterranean: Characteristics, trends and links to large-scale patterns. *Nat. Hazards Earth Syst. Sci.* **2010**, *10*, 1379–1391. [\[CrossRef\]](#)
- Mariotti, A.; Ning, Z.; Lau, K.-M. Euro-Mediterranean rainfall and ENSO, a seasonally varying relationship. *Geophys. Res. Lett.* **2002**, *29*, 1621. [\[CrossRef\]](#)
- López-Parages, J.; Rodríguez-Fonseca, B. Multidecadal modulation of El Niño influence on the Euro-Mediterranean rainfall. *Geophys. Res. Lett.* **2012**, *39*, L02704. [\[CrossRef\]](#)

17. Henriksson, S.V. Interannual oscillations and sudden shifts in observed and modeled climate. *Atmos. Sci. Lett.* **2018**, *19*, e850. [[CrossRef](#)]
18. Turki, I.; Massei, N.; Laignel, B.; Shafiei, H. Effects of Global Climate Oscillations on Intermonthly to Interannual Variability of Sea levels along the English Channel Coasts (NW France). *Oceanologia* **2020**, *62*, 226–242. [[CrossRef](#)]
19. Giuntoli, I.; Fabiano, F.; Corti, S. Seasonal predictability of Mediterranean weather regimes in the Copernicus C3S systems. *Clim. Dyn.* **2022**, *58*, 2131–2147. [[CrossRef](#)]
20. Zampieri, M.; Toreti, A.; Schindler, A.; Scoccimarro, E.; Gualdi, S. Atlantic multi-decadal oscillation influence on weather regimes over Europe and the Mediterranean in spring and summer. *Glob. Planet. Chang.* **2017**, *151*, 92–100. [[CrossRef](#)]
21. Merino-Martín, L.; Moreno-de las Heras, M.; Espigares, T.; Nicolau, J.M. Overland flow directs soil moisture and ecosystem processes at patch scale in Mediterranean restored hillslopes. *Catena* **2015**, *133*, 71–84. [[CrossRef](#)]
22. Kim, G.U.; Seo, K.H.; Chen, D. Climate change over the Mediterranean and current destruction of marine ecosystem. *Sci. Rep.* **2019**, *9*, 18813. [[CrossRef](#)] [[PubMed](#)]
23. Chagas, V.B.P.; Chaffe, P.L.B.; Blöschl, G. Climate and land management accelerate the Brazilian water cycle. *Nat. Commun.* **2022**, *13*, 5136. [[CrossRef](#)] [[PubMed](#)]
24. Moatti, J.P.; Thiébault, S. *The Mediterranean Region under Climate Change*, 1st ed.; IRD Éditions: Marseille, France, 2018; 736p. [[CrossRef](#)]
25. Hansen, W.D.; Schwartz, N.B.; Williams, A.P.; Albrich, K.; Kueppers, L.M.; Rammig, A.; Reyer, C.P.O.; Staver, A.C.; Seidl, R. Global forests are influenced by the legacies of past inter-annual temperature variability. *Environ. Res. Ecol.* **2022**, *1*, 011001. [[CrossRef](#)]
26. White, E.E.; Ury, E.A.; Bernhardt, E.S.; Yang, X. Climate Change Driving Widespread Loss of Coastal Forested Wetlands Throughout the North American Coastal Plain. *Ecosystems* **2022**, *25*, 812–827. [[CrossRef](#)]
27. Anaya-Romero, M.; Muñoz-Rojas, M.; Ibáñez, B.; Marañón, T. Evaluation of forest ecosystem services in Mediterranean areas. A regional case study in South Spain. *Ecosyst. Serv.* **2016**, *20*, 82–90. [[CrossRef](#)]
28. Tammi, I.; Mustajärvi, K.; Rasinmäki, J. Integrating spatial valuation of ecosystem services into regional planning and development. *Ecosyst. Serv.* **2017**, *26 Pt B*, 329–344. [[CrossRef](#)]
29. Inostroza, L.; König, H.J.; Pickard, B.; Zhen, L. Putting ecosystem services into practice: Trade-off assessment tools, indicators and decision support systems. *Ecosyst. Serv.* **2017**, *26 Pt B*, 303–305. [[CrossRef](#)]
30. Mann, C.; Loft, L.; Hansjürgens, B. Governance of Ecosystem Services: Lessons learned for sustainable institutions. *Ecosyst. Serv.* **2015**, *16*, 275–281. [[CrossRef](#)]
31. De Stefano, L.; Hernández-Mora, N.; Iglesias, A.; Sánchez, B. Water for rice farming and biodiversity: Exploring choices for adaptation to climate change in Doñana, southern Spain. In *Adaptation to Climate Change through Water Resources Management: Capacity, Equity, and Sustainability*, 1st ed.; Stucker, D., Lopez-Gunn, E., Eds.; Routledge/Earthscan: Oxford, UK, 2014; Volume 1, pp. 1–22. Available online: https://www.researchgate.net/publication/264991601_Water_for_rice_farming_and_biodiversity_Exploring_choices_for_adaptation_to_climate_change_in_Donana_southern_Spain (accessed on 25 November 2022).
32. Regos, A.; Tapia, L.; Arenas-Castro, S.; Domínguez, J. Ecosystem Functioning Influences Species Fitness at Upper Trophic Levels. *Ecosystems* **2022**, *25*, 1037–1051. [[CrossRef](#)]
33. Sumner, G.; Homar, V.; Ramis, C. Precipitation seasonality in eastern and southern coastal Spain. *Int. J. of Climatol.* **2001**, *21*, 219–247. [[CrossRef](#)]
34. Ruiz-Sinoga, J.D.; Garcia-Marín, R.; Martínez-Murillo, J.F.; Gabarron-Galeote, M.A. Precipitation dynamics in southern Spain: Trends and cycles. *Int. J. Climatol.* **2011**, *35*, 2281–2289. [[CrossRef](#)]
35. Brown, C.L.; Coe, P.K.; Clark, D.A.; Wisdom, M.J.; Rowland, M.M.; Averett, J.P.; Johnson, B.K. Climate change effects on understory plant phenology: Implications for large herbivore forage availability. *Environ. Res. Ecol.* **2022**, *1*, 011002. [[CrossRef](#)]
36. Yeakley, J.A.; Moen, R.A.; Breshears, D.D.; Nungesser, M.K. Response of North American ecosystem models to multi-annual periodicities in temperature and precipitation. *Landsc. Ecol.* **1994**, *9*, 249–260. [[CrossRef](#)]
37. Loehle, C. Disequilibrium and relaxation times for species responses to climate change. *Ecol. Model.* **2018**, *384*, 23–29. [[CrossRef](#)]
38. Zhang, R.; Guo, J.; Liang, T.; Feng, Q. Grassland vegetation phenological variations and responses to climate change in the Xinjiang region, China. *Quat. Int.* **2019**, *513*, 56–65. [[CrossRef](#)]
39. Ye, Y.; Zhang, X. Exploration of global spatiotemporal changes of fall foliage coloration in deciduous forests and shrubs using the VIIRS land surface phenology product. *Sci. Remote Sens.* **2021**, *4*, 100030. [[CrossRef](#)]
40. Mulomba-Mukadi, P.; González-García, C. Time Series Analysis of Climatic Variables in Peninsular Spain. Trends and Forecasting Models for Data between 20th and 21st Centuries. *Climate* **2021**, *9*, 119. [[CrossRef](#)]
41. Bohn, F.J.; Frank, K.; Huth, A. Of climate and its resulting tree growth: Simulating the productivity of temperate forests. *Ecol. Model.* **2014**, *278*, 9–17. [[CrossRef](#)]
42. Vinnikov, K.Y.; Groisman, P.Y.; Lugina, K.M. Empirical Data on Contemporary Global Climate Changes (Temperature and Precipitation). *J. Clim.* **1990**, *3*, 662–677. [[CrossRef](#)]
43. Wanishsakpong, W.; Owusu, B.E. Optimal Time Series Model for Forecasting Monthly Temperature in the Southwestern Region of Thailand. *Model. Earth Syst. Environ.* **2020**, *6*, 525–532. [[CrossRef](#)]

44. González-Hidalgo, J.C.; Lopez-Bustins, J.A.; Stepánek, P.; Martin-Vide, J.; De Luis, M. Monthly Precipitation Trends on the Mediterranean Fringe of the Iberian Peninsula during the Second Half of the Twentieth Century (1951–2000). *Int. J. Climatol.* **2009**, *29*, 1415–1429. [[CrossRef](#)]
45. Romero, R.; Guijarro, J.A.; Alonso, S. A 30-Year (1964–1993) Daily Rainfall Data Base for the Spanish Mediterranean Regions: First Exploratory Study. *Int. J. Climatol.* **1998**, *18*, 541–560. [[CrossRef](#)]
46. Zhou, J.; Cai, W.; Qin, Y.; Lai, L.; Guan, T.; Zhang, X.; Jiang, L.; Du, H.; Yang, D.; Cong, Z.; et al. Alpine vegetation phenology dynamic over 16years and its covariation with climate in a semi-arid region of China. *Sci. Total Environ.* **2016**, *572*, 119–128. [[CrossRef](#)] [[PubMed](#)]
47. Ayuga, E.; González, C.; Montero, M.J.; Robredo, J.C. Statistical Models of ARIMA Prediction of Precipitation in Two Spanish Stations Representative of two Groups with Different Climatic Characteristics. In *Regional Climate Change and Its Impacts*, 1st ed.; Rodríguez, J.S., India, M.B., Anfrons, E.A., Eds.; Spanish Society of Climatology: Tarragona, Spain, 2008; Volume 6 (Serie A), pp. 15–24. Available online: <http://hdl.handle.net/20.500.11765/8544> (accessed on 25 November 2022).
48. Del Río, S.; Herrero, L.; Pinto-Gomes, C.; Penas, A. Spatial Analysis of Mean Temperature Trends in Spain over the Period 1961–2006. *Glob. Planet. Chang.* **2011**, *78*, 65–75. [[CrossRef](#)]
49. McKee, T.B.; Doesken, N.J.; Kleist, J. Drought monitoring with multiple time scales. In Proceedings of the Ninth Conference on Applied Climatology, Anaheim, CA, USA, 17–22 January 1993; pp. 233–236. Available online: <https://climate.colostate.edu/pdfs/relationshipofdroughtfrequency.pdf> (accessed on 25 November 2022).
50. Moreira, E.E.; Martins, D.S.; Pereira, L.S. Assessing drought cycles in SPI time series using a Fourier analysis. *Nat. Hazards Earth Syst. Sci.* **2015**, *15*, 571–585. [[CrossRef](#)]
51. Hosseinzadeh, A.; Seyedkaboli, H.; Zarei, H.; Akhoond-ali, A.-M.; Farjad, B. Impact of climate change on the severity, duration, and frequency of drought in a semi-arid agricultural basin. *Geoenviron. Disasters* **2015**, *2*, 1–9. [[CrossRef](#)]
52. Tirivarombo, S.; Osupile, D.; Eliasson, P. Drought monitoring and analysis: Standardised Precipitation Evapotranspiration Index (SPEI) and Standardised Precipitation Index (SPI). *Phys. Chem. Earth Parts A/B/C* **2018**, *106*, 1–10. [[CrossRef](#)]
53. Tigkas, D.; Vangelis, H.; Tsakiris, G. Drought characterisation based on an agriculture-oriented standardised precipitation index. *Theor. Appl. Climatol.* **2019**, *135*, 1435–1447. [[CrossRef](#)]
54. MODIS (Moderate Resolution Imaging Spectroradiometer). Available online: <https://modis.gsfc.nasa.gov/> (accessed on 4 October 2022).
55. Li, Z.; Huffman, T.; McConkey, B.; Townley-Smith, L. Monitoring and modeling spatial and temporal patterns of grassland dynamics using time-series MODIS NDVI with climate and stocking data. *Remote Sens. Environ.* **2013**, *138*, 232–244. [[CrossRef](#)]
56. Rossini, M.; Migliavacca, M.; Galvagno, M.; Meroni, M.; Cogliati, S.; Cremonese, E.; Fava, F.; Gitelson, A.; Julitta, T.; Morra di Cella, U. Remote estimation of grassland gross primary production during extreme meteorological seasons. *Int. J. Appl. Earth Obs. Geoinf.* **2014**, *29*, 1–10. [[CrossRef](#)]
57. Vijith, H.; Dodge-Wan, D. Applicability of MODIS land cover and Enhanced Vegetation Index (EVI) for the assessment of spatial and temporal changes in strength of vegetation in tropical rainforest region of Borneo. *Remote Sens. Appl. Soc. Environ.* **2020**, *18*, 100311. [[CrossRef](#)]
58. Naghdizadegan-Jahromi, M.; Naghdyzadegan-Jahromi, M.; Pourghasemi, H.-M.; Zand-Parsa, S.; Jamshidi, S. Chapter 12—Accuracy assessment of forest mapping in MODIS land cover dataset using fuzzy set theory. In *Forest Resources Resilience and Conflicts*, 1st ed.; Pravat Kumar Shit, P.-K., Pourghasemi, H.-M., Adhikary, P.-P., Bhunia, G.-S., Sati, V.-P., Eds.; Elsevier: Amsterdam, The Netherlands, 2021; pp. 165–183. [[CrossRef](#)]
59. Izadi, S.; Sohrabi, H. Chapter 14—Using Bayesian kriging and satellite images to estimate above-ground biomass of Zagros mountainous forests. In *Forest Resources Resilience and Conflicts*, 1st ed.; Pravat Kumar Shit, P.-K., Pourghasemi, H.-M., Adhikary, P.-P., Bhunia, G.-S., Sati, V.-P., Eds.; Elsevier: Amsterdam, The Netherlands, 2021; pp. 193–201. [[CrossRef](#)]
60. Cui, B.; Zhao, Q.; Huang, W.; Song, X.; Ye, H.; Zhou, X. A New Integrated Vegetation Index for the Estimation of Winter Wheat Leaf Chlorophyll Content. *Remote Sens.* **2019**, *11*, 974. [[CrossRef](#)]
61. Kira, O.; Linker, R.; Gitelson, A. No destructive estimation of foliar chlorophyll and carotenoid contents Focus on informative spectral bands. *Int. J. Appl. Earth Obs. Geoinf.* **2015**, *38*, 251–260. [[CrossRef](#)]
62. Gallardo, J.L.; Pompa, M. Detecting Individual Tree Attributes and Multispectral Indices Using Unmanned Aerial Vehicles: Applications in a Pine Clonal Orchard. *Remote Sens.* **2020**, *12*, 4144. [[CrossRef](#)]
63. Dennison, P.E. Corresponding author, Roberts, D.A.; Peterson, S.H.; Rechel, J. Use of Normalized Difference Water Index for monitoring live fuel moisture. *Int. J. Remote Sens.* **2005**, *26*, 1035–1042. [[CrossRef](#)]
64. Hardy, C.C.; Burgan, R.E. Evaluation of NDVI for monitoring live moisture in three vegetation types of the Western U.S. *Photogramm. Eng. Remote Sens.* **1999**, *65*, 603–610. Available online: https://www.asprs.org/wp-content/uploads/pers/1999journal/may/1999_may_603-610.pdf (accessed on 20 August 2022).
65. Chuvieco, E.; Riaño, D.; Aguado, I.; Cocero, D. Estimation of fuel moisture content from multitemporal analysis of Landsat Thematic Mapper reflectance data: Applications in fire danger assessment. *Int. J. Remote Sens.* **2002**, *23*, 2145–2162. [[CrossRef](#)]
66. Ren, H.; Zhou, G. Estimating green biomass ratio with remote sensing in arid grasslands. *Ecol. Indic.* **2019**, *98*, 568–574. [[CrossRef](#)]
67. Ullah, S.; Si, Y.; Schlerf, M.; Skidmore, A.K.; Shafique, M.; Iqbal, I.A. Estimation of grassland biomass and nitrogen using MERIS data. *Int. J. Appl. Earth Obs. Geoinf.* **2012**, *19*, 196–204. [[CrossRef](#)]

68. Peñuelas, J.; Baret, F.; Filella, I. Semi-empirical indices to assess carotenoids/chlorophyll a ratio from leaf spectral reflectance. *Photosynthetica* **1995**, *31*, 221–230.
69. Baret, F.; Clevers, J.G.P.W.; Steven, M.D. The robustness of canopy gap fraction estimates from red and near-infrared reflectances: A comparison of approaches. *Remote Sens. Environ.* **1995**, *54*, 141–151. [[CrossRef](#)]
70. Yang, F.; Sun, J.; Fang, H.; Yao, Z.; Zhang, J.; Zhu, Y.; Song, K.; Wang, Z.; Hu, M. Comparison of different methods for corn LAI estimation over northeastern China. *Int. J. Appl. Earth Obs. Geoinf.* **2012**, *18*, 462–471. [[CrossRef](#)]
71. Nguy-Robertson, A.L.; Peng, Y.; Gitelson, A.A.; Arkebauer, T.J.; Pimstein, A.; Herrmann, I.; Karnieli, A.; Rundquist, D.C.; Bonfil, D.J. Estimating green LAI in four crops: Potential of determining optimal spectral bands for a universal algorithm. *Agric. For. Meteorol.* **2014**, *192–193*, 140–148. [[CrossRef](#)]
72. Darvishzadeh, R.; Atzberger, C.; Skidmore, A.; Schlerf, M. Mapping grassland leaf area index with airborne hyperspectral imagery: A comparison study of statistical approaches and inversion of radiative transfer models. *ISPRS J. Photogramm. Remote Sens.* **2011**, *66*, 894–906. [[CrossRef](#)]
73. Feng, W.; Wu, Y.; He, L.; Ren, X.; Wang, Y.; Hou, G.; Wang, Y.; Liu, W.; Guo, T. An optimized non-linear vegetation index for estimating leaf area index in winter wheat. *Precision Agric.* **2019**, *20*, 1157–1176. [[CrossRef](#)]
74. Zhang, F.; Zhou, G. Estimation of Canopy Water Content by Means of Hyperspectral Indices Based on Drought Stress Gradient Experiments of Maize in the North Plain China. *Remote Sens.* **2015**, *7*, 15203–15223. [[CrossRef](#)]
75. Granero-Belinchón, C.; Adeline, K.; Lemonsu, A.; Briottet, X. Phenological Dynamics Characterization of Alignment Trees with Sentinel-2 Imagery: A Vegetation Indices Time Series Reconstruction Methodology Adapted to Urban Areas. *Remote Sens.* **2020**, *12*, 639. [[CrossRef](#)]
76. Di Bella, C.M.; Paruelo, J.M.; Becerra, J.E.; Bacour, C.; Baret, F. Effect of senescent leaves on NDVI-based estimates of APAR: Experimental and modelling evidence. *Int. J. Remote Sens.* **2004**, *25*, 5415–5427. [[CrossRef](#)]
77. Zhang, Y.; Xiao, X.; Jin, C.; Dong, J.; Zhou, Z.; Wagle, P.; Joiner, J.; Guanter, L.; Zhang, Y.; Zhang, G.; et al. Consistency between sun-induced chlorophyll fluorescence and gross primary production of vegetation in North America. *Remote Sens. Environ.* **2016**, *183*, 154–169. [[CrossRef](#)]
78. He, M.; Ju, W.; Zhou, Y.; Chen, J.; He, H.; Wang, S.; Wang, H.; Guan, D.; Yan, Y.; Li, Y.; et al. Development of a two-leaf light use efficiency model for improving the calculation of terrestrial gross primary productivity. *Agric. For. Meteorol.* **2013**, *173*, 28–39. [[CrossRef](#)]
79. Piao, S.; Mohammat, A.; Fang, J.; Cai, Q.; Feng, J. NDVI-based increase in growth of temperate grasslands and its responses to climate changes in China. *Glob. Environ. Chang.* **2006**, *16*, 340–348. [[CrossRef](#)]
80. Bastin, G.; Scarth, P.; Chewings, V.; Sparrow, A.; Denham, R.; Schmidt, M.; O'Reagain, P.; Shepherd, R.; Abbott, B. Separating grazing and rainfall effects at regional scale using remote sensing imagery: A dynamic reference-cover method. *Remote Sens. Environ.* **2012**, *121*, 443–457. [[CrossRef](#)]
81. Hernández-Clemente, R.; Navarro-Cerrillo, R.M.; Zarco-Tejada, P.J. Carotenoid content estimation in a heterogeneous conifer forest using narrow-band indices and PROSPECT+DART simulations. *Remote Sens. Environ.* **2012**, *127*, 298–315. [[CrossRef](#)]
82. Cui, F.; Wang, B.; Zhang, Q.; Tang, H.; De Maeyer, P.H.; Hamdi, R.; Dai, L. Climate change versus land-use change—What affects the ecosystem services more in the forest-steppe ecotone? *Sci. Total Environ.* **2021**, *759*, 143525. [[CrossRef](#)]
83. Daneshi, A.; Brouwer, R.; Najafinejad, A.; Panahi, M.; Zareandian, A.; Maghsood, F.F. Modelling the impacts of climate and land use change on water security in a semi-arid forested watershed using InVEST. *J. Hydrol.* **2021**, *593*, 125621. [[CrossRef](#)]
84. Tomaz, C.; Alegria, C.; Massano, J.; Canavarro, M. Land cover change and afforestation of marginal and abandoned agricultural land: A 10 year analysis in a Mediterranean region. *For. Ecol. Manag.* **2013**, *308*, 40–49. [[CrossRef](#)]
85. Ferrara, A.; Salvati, L.; Sabbi, A.; Colantoni, A. Soil resources, land cover changes and rural areas: Towards a spatial mismatch? *Sci. Total Environ.* **2014**, *478*, 116–122. [[CrossRef](#)]
86. Luo, Y.; Lü, Y.; Liua, L.; Liang, H.; Li, T.; Ren, Y. Spatiotemporal scale and integrative methods matter for quantifying the driving forces of land cover change. *Sci. Total Environ.* **2020**, *739*, 139622. [[CrossRef](#)]
87. De Luis, M.; Vicente, S.M.; González-Hidalgo, J.C.; Raventós, J. Application of Contingency Tables (Cross-Tab-Analysis) to the Spatial Analysis of Climate Trends in the Eastern Sector of the Iberian Peninsula. *Cuad. Investig. Geogr.* **2003**, *29*, 23–34. [[CrossRef](#)]
88. Requena-Mullor, J.M.; Quintas-Soriano, C.; Brandt, J.; Cabello, J.; Castro, A.J. Modeling how land use legacy affects the provision of ecosystem services in Mediterranean southern Spain. *Environ. Res. Lett.* **2018**, *13*, 114008. [[CrossRef](#)]
89. Wang, J.; Zhang, X.; Rodman, K. Land cover composition, climate, and topography drive land surface phenology in a recently burned landscape: An application of machine learning in phenological modeling. *Agric. For. Meteorol.* **2021**, *304–305*, 108432. [[CrossRef](#)]
90. Senf, C. Seeing the System from Above: The Use and Potential of Remote Sensing for Studying Ecosystem Dynamics. *Ecosystems* **2022**, *25*, 1719–1737. [[CrossRef](#)]
91. Zhu, Z.; Wulder, M.A.; Roy, D.P.; Woodcock, C.E.; Hansen, M.C.; Radeloff, W.C.; Healey, S.P.; Schaaf, C.; Hostert, P.; Strobl, P.; et al. Benefits of the free and open Landsat data policy. *Remote Sens. Environ.* **2019**, *224*, 382–385. [[CrossRef](#)]
92. Zhao, Y.; Wang, X.; Novillo, C.J.; Arrogante-Funes, P.; Vázquez-Jiménez, R.; Maestre, F.T. Albedo estimated from remote sensing correlates with ecosystem multifunctionality in global drylands. *J. Arid. Environ.* **2018**, *157*, 116–123. [[CrossRef](#)]
93. Qader, S.H.; Atkinson, P.M.; Dash, J. Spatiotemporal variation in the terrestrial vegetation phenology of Iraq and its relation with elevation. *Int. J. Appl. Earth Obs. Geoinf.* **2015**, *41*, 107–117. [[CrossRef](#)]

94. Shtiliyanova, A.; Bellocchi, G.; Borrás, D.; Eza, U.; Martín, R.; Carrère, P. Kriging-based approach to predict missing air temperature data. *Comput. Electron. Agric.* **2017**, *142 Pt A*, 440–449. [[CrossRef](#)]
95. Nistor, M.-M. Groundwater vulnerability in Europe under climate change. *Quat. Int.* **2020**, *547*, 185–196. [[CrossRef](#)]
96. Swetnam, R.D.; Harrison-Curran, S.K.; Smith, G.R. Quantifying visual landscape quality in rural Wales: A GIS-enabled method for extensive monitoring of a valued cultural ecosystem service. *Ecosyst. Serv.* **2017**, *26 Pt B*, 451–464. [[CrossRef](#)]
97. Domingo-Marimon, C.; Masó, J.; Prat, E.; Zabala, A.; Serral, I.; Batalla, M.; Ninyerola, M.; Cristóbal, J. Aligning citizen science and remote sensing phenology observations to characterize climate change impact on vegetation. *Environ. Res. Lett.* **2022**, *17*, 085007. [[CrossRef](#)]
98. Baldocchi, D.; Falge, E.; Gu, L.; Olson, R.; Hollinger, D.; Running, S.; Anthoni, P.; Bernhofer, C.H.; Davis, K.; Evans, R.; et al. FLUXNET: A New Tool to Study the Temporal and Spatial Variability of Ecosystem-Scale Carbon Dioxide, Water Vapor, and Energy Flux Density. *Bull. Am. Meteorol. Soc.* **2001**, *82*, 2415–2434. [[CrossRef](#)]
99. Ruiz-Benito, P.; Vacchiano, G.; Lines, E.M.; Reyer, C.P.O.; Ratcliffe, S.; Morin, X.; Hartig, F.; Mäkelä, A.; Yousefpour, R.; Chaves, J.E.; et al. Available and missing data to model impact of climate change on European forests. *Ecol. Model.* **2020**, *416*, 108870. [[CrossRef](#)]
100. Zhang, T.; Li, J.; Liu, Q.; Huang, Q. A cloud-enabled remote visualization tool for time-varying climate data analytics. *Environ. Model. Softw.* **2016**, *75*, 513–518. [[CrossRef](#)]
101. Harris, R.; Baumann, I. Open data policies and satellite Earth observation. *Space Policy* **2015**, *32*, 44–53. [[CrossRef](#)]
102. Donager, J.; Sankey, T.T.; Sánchez-Meador, A.J.; Sankey, J.B.; Springer, A. Integrating airborne and mobile lidar data with UAV photogrammetry for rapid assessment of changing forest snow depth and cover. *Sci. Remote Sens.* **2021**, *4*, 100029. [[CrossRef](#)]
103. Del Río, S.; Herrero, L.; Fraile, R.; Penas, A. Spatial distribution of recent rainfall trends in Spain (1961–2006). *Int. J. Climatol.* **2011**, *31*, 656–667. [[CrossRef](#)]
104. Martínez-Artigas, J.; Lemus-Canovas, M.; López-Bustins, J.A. Precipitation in peninsular Spain: Influence of teleconnection indices and spatial regionalization. *Int. J. Climatol.* **2021**, *41*, E1320–E1335. [[CrossRef](#)]
105. González-Hidalgo, J.C.; Vicente-Serrano, S.M.; Peña-Angulo, D.; Salinas, C.; Tomas-Burguera, M.; Beguería, S. High-resolution spatio-temporal analyses of drought episodes in the western Mediterranean basin (Spanish mainland, Iberian Peninsula). *Acta Geophys.* **2018**, *66*, 381–392. [[CrossRef](#)]
106. Vélez-Nicolás, M.; García-López, S.; Ruiz-Ortiz, V.; Zazo, S.; Molina, J.L. Precipitation Variability and Drought Assessment Using the SPI: Application to Long-Term Series in the Strait of Gibraltar Area. *Water* **2022**, *14*, 884. [[CrossRef](#)]
107. Guttman, N.B. On the sensitivity of sample L moments to sample size. *J. Clim.* **1994**, *7*, 1026–1029. [[CrossRef](#)]
108. Guttman, N.B. Comparing the Palmer drought index and the Standardized Precipitation Index. *J. Am. Water Resour. Assoc.* **1998**, *34*, 113–121. [[CrossRef](#)]
109. Guttman, N.B. Accepting the Standardized Precipitation Index: A calculation algorithm. *J. Am. Water Resour. Assoc.* **1999**, *35*, 311–322. [[CrossRef](#)]
110. Vicente-Serrano, S.M.; Tomas-Burguera, M.; Beguería, S.; Reig, F.; Latorre, B.; Peña-Gallardo, M.; Luna, M.Y.; Morata, A.; González-Hidalgo, J.C. A High Resolution Dataset of Drought Indices for Spain. *Data* **2017**, *2*, 22. [[CrossRef](#)]
111. Yaffee, S.L. Three Faces of Ecosystem Management. *Conserv. Biol.* **1998**, *13*, 713–725. [[CrossRef](#)]
112. Ludwig, J.A.; Tongway, D.J.; Bastin, G.N.; James, C.D. Monitoring ecological indicators of rangeland functional integrity and their relation to biodiversity at local to regional scales. *Austral Ecol.* **2004**, *29*, 108–120. [[CrossRef](#)]
113. Constanza, R.; d’Arge, R.; Groot, R.; Farber, S.; Grasso, M.; Hannon, B.; Limburg, K.; Naeem, S.; O’Neil, R.V.; Paruelo, J.; et al. The value of the world’s ecosystem services and natural capital. *Nature* **1997**, *387*, 253–260. [[CrossRef](#)]
114. Grumbine, R.E. What is ecosystem management? *Conserv. Biol.* **1994**, *8*, 27–38. [[CrossRef](#)]
115. Halpin, P.N. Global climate change and natural-area protection: Management responses and research directions. *Ecol. Appl.* **1997**, *3*, 828–843. [[CrossRef](#)]
116. Grantham, H.S.; Bode, M.; McDonald-Madden, E.; Game, E.T.; Knight, A.T.; Possingham, H.P. Effective conservation planning requires learning and adaptation. *Front. Ecol. Environ.* **2010**, *8*, 431–437. [[CrossRef](#)]
117. Lindenmayer, D.B.; Likens, G.E. The science and application of ecological monitoring. *Biol. Conserv.* **2010**, *143*, 1317–1328. [[CrossRef](#)]
118. Wenzel, B. Organizing coordination for an ecosystem approach to marine research and management advice: The case of ICES. *Mar. Policy* **2017**, *82*, 138–146. [[CrossRef](#)]
119. Martínez-Murillo, J.F.; Senciales González, J.M. Morphogenesis and soil processes. The case of the Montes de Málaga. *Baetica* **2003**, *25*, 219–258. [[CrossRef](#)]
120. Edwards, D.C.; McKee, T.B. Characteristics of 20th Century Drought in the United States at Multiple Time Scales. Climatology Report 97-2, 1997, Department of Atmospheric Science, Colorado State University, Fort Collins. Available online: <https://mountainscholar.org/handle/10217/170176?show=full> (accessed on 5 October 2022).
121. Karanja, A.; Ondimu, K.; Recha, C. Analysis of Temporal Drought Characteristic Using SPI Drought Index Based on Rainfall Data in Laikipia West Sub-County, Kenya. *Open Access Libr. J.* **2017**, *4*, e3765. [[CrossRef](#)]
122. Gumus, V.; Simsek, O.; Avsaroglu, Y.; Agun, B. Spatio-temporal trend analysis of drought in the GAP Region, Turkey. *Nat. Hazards* **2021**, *109*, 1759–1776. [[CrossRef](#)]

123. Vicente-Serrano, S.M.; Domínguez-Castro, F.; Murphy, C.; Hannaford, J.; Reig, F.; Peña-Angulo, D.; Trambly, Y.; Trigo, R.M.; Mac Donald, N.; Luna, M.Y.; et al. Long-term variability and trends in meteorological droughts in Western Europe (1851–2018). *Int. J. Climatol.* **2021**, *41* (Suppl. 1), E690–E717. [CrossRef]
124. Haboudane, D.; Miller, J.R.; Pattey, E.; Zarco-Tejada, P.J.; Strachane, I.A. Hyperspectral vegetation indices and novel algorithms for predicting green LAI of crop canopies: Modeling and validation in the context of precision agriculture. *Remote Sens. Environ.* **2004**, *90*, 337–352. [CrossRef]
125. Schlemmer, M.; Gitelson, A.; Schepers, J.; Ferguson, R.; Peng, Y.; Shanahana, J.; Rundquist, R. Remote estimation of nitrogen and chlorophyll contents in maize at leaf and canopy levels. *Int. J. Appl. Earth Obs. Geoinf.* **2013**, *25*, 47–54. [CrossRef]
126. Marino, S.; Alvino, A. Vegetation Indices Data Clustering for Dynamic Monitoring and Classification of Wheat Yield Crop Traits. *Remote Sens.* **2021**, *13*, 541. [CrossRef]
127. Rouse, J.W.; Haas, R.H.; Schell, J.A.; Deering, D.W.; Harlan, J.C. *Monitoring the Vernal Advancements and Retrogradation of Natural Vegetation*; Final Report; NASA/GSFC: Greenbelt, MD, USA, 1973; pp. 1–137. Available online: <https://www.semanticscholar.org/paper/Monitoring-the-Vernal-Advancement-and-Green-Wave-Rouse-Haas/c3a30c40d304a7a312942c0c243f5033b8c3fd3f> (accessed on 29 August 2022).
128. Baret, F.; Guyot, G. Potentials and limits of vegetation indices for LAI and APAR assessment. *Remote Sens. Environ.* **1991**, *35*, 161–173. [CrossRef]
129. Jordan, C.F. Derivation of Leaf-Area Index from Quality of Light on the Forest Floor. *Ecology* **1969**, *50*, 663–666. [CrossRef]
130. Rouse, J.W.; Haas, R.H.; Schell, J.A.; Deering, D.W. *Monitoring Vegetation Systems in the Great Plains with ERTS, Third ERTS Symposium*; NASA: Washington, DC, USA, 1973; pp. 309–317. Available online: [https://books.google.es/books?hl=es&lr=&id=bn_xAAAAMAAJ&oi=fnd&pg=PA309&dq=Rouse,+J.+W.%3B+Haas,+R.+H.%3B+Schell,+J.+A.%3B+Deering,+D.+W.+Monitoring+Vegetation+Systems+in+the+Great+Plains+with+ERTS,+Third+ERTS+Symposium+\(Washinton,+DC:+NASA\),+1973,+pp.+309%E2%80%93317.&ots=YTLsLGBUKJ&sig=fjUfMVyayU88xSO5KZuavcqQk0#v=onepage&q&f=false](https://books.google.es/books?hl=es&lr=&id=bn_xAAAAMAAJ&oi=fnd&pg=PA309&dq=Rouse,+J.+W.%3B+Haas,+R.+H.%3B+Schell,+J.+A.%3B+Deering,+D.+W.+Monitoring+Vegetation+Systems+in+the+Great+Plains+with+ERTS,+Third+ERTS+Symposium+(Washinton,+DC:+NASA),+1973,+pp.+309%E2%80%93317.&ots=YTLsLGBUKJ&sig=fjUfMVyayU88xSO5KZuavcqQk0#v=onepage&q&f=false) (accessed on 26 August 2022).
131. Jiang, Z.; Huete, A.R.; Chen, J.; Chen, Y.; Li, J.; Yan, G.; Zhang, X. Analysis of NDVI and scaled difference vegetation index retrievals of vegetation fraction. *Remote Sens. Environ.* **2006**, *101*, 366–378. [CrossRef]
132. Chang, A.; Yeom, J.; Jung, J.; Landivar, J. Comparison of Canopy Shape and Vegetation Indices of Citrus Trees Derived from UAV Multispectral Images for Characterization of Citrus Greening Disease. *Remote Sens.* **2020**, *12*, 4122. [CrossRef]
133. Modica, G.; Messina, C.; De Luca, G.; Fiozzo, V.; Praticò, S. Monitoring the vegetation vigor in heterogeneous citrus and olive orchards. A multiscale object-based approach to extract trees' crowns from UAV multispectral imagery. *Comput. Electron. Agric.* **2020**, *175*, 105500. [CrossRef]
134. Viskovic, L.; Kosovic, I.N.; Mastelic, T. Crop Classification using Multi-spectral and Multitemporal Satellite Imagery with Machine Learning. In Proceedings of the 2019 International Conference on Software, Telecommunications and Computer Networks (SoftCOM), Split, Croatia, 19–21 September 2019; pp. 1–5. [CrossRef]
135. Costa, L.; Nunes, L.; Ampatzidis, Y. A new visible band index (vNDVI) for estimating NDVI values on RGB images utilizing genetic algorithms. *Comput. Electron. Agric.* **2020**, *172*, 105334. [CrossRef]
136. Chen, J.M. Evaluation of vegetation indices and modified simple ratio for boreal applications. *Can. J. Remote Sens.* **1996**, *22*, 229–242. [CrossRef]
137. Campos, J.C.; Sillero, N.; Brito, J.C. Normalized difference water indexes have dissimilar performances in detecting seasonal and permanent water in the Sahara-Sahel transition zone. *J. Hydrol.* **2012**, *464–465*, 438–446. [CrossRef]
138. Doña, C.; Morant, D.; Picazo, A.; Rochera, C.; Sánchez, J.M.; Camacho, A. Estimation of Water Coverage in Permanent and Temporary Shallow Lakes and Wetlands by Combining Remote Sensing Techniques and Genetic Programming: Application to the Mediterranean Basin of the Iberian Peninsula. *Remote Sens.* **2021**, *13*, 652. [CrossRef]
139. Gao, B.-C. NDWI—A normalized difference water index for remote sensing of vegetation liquid water from space. *Remote Sens. Environ.* **1996**, *58*, 257–266. [CrossRef]
140. Jackson, T.J.; Chen, D.; Cosh, M.; Li, F.; Anderson, M.; Walthall, C.; Doriaswamy, P.; Hunt, E.R. Vegetation water content mapping using Landsat data derived normalized difference water index for corn and soybeans. *Remote Sens. Environ.* **2004**, *92*, 475–482. [CrossRef]
141. McFeeters, S.K. The use of the Normalized Difference Water Index (NDWI) in the delineation of open water features. *Int. J. Remote Sens.* **1996**, *17*, 1425–1432. [CrossRef]
142. Xu, H. Modification of normalised difference water index (NDWI) to enhance open water features in remotely sensed imagery. *Int. J. Remote Sens.* **2006**, *27*, 3025–3033. [CrossRef]
143. Phompila, C.; Lewis, M.; Ostendorf, B.; Clarke, K. MODIS EVI and LST Temporal Response for Discrimination of Tropical Land Covers. *Remote Sens.* **2015**, *7*, 6026–6040. [CrossRef]
144. Matsushita, B.; Yang, W.; Chen, J.; Onda, Y.; Qiu, G. Sensitivity of the Enhanced Vegetation Index (EVI) and Normalized Difference Vegetation Index (NDVI) to Topographic Effects: A Case Study in High-density Cypress Forest. *Sensors* **2007**, *7*, 2636–2651. [CrossRef] [PubMed]
145. Villamuelas, M.; Fernández, N.; Albanell, E.; Gálvez-Cerón, A.; Bartolomé, J.; Mentaberre, G.; López-Olvera, J.R.; Fernández-Aguilar, X.; Colom-Cadena, A.; López-Martín, J.M.; et al. The Enhanced Vegetation Index (EVI) as a proxy for diet quality and composition in a mountain ungulate. *Ecol. Indic.* **2016**, *61 Pt 2*, 658–666. [CrossRef]

146. Gurung, R.B.; Breidt, F.J.; Dutin, A.; Ogle, E.M. Predicting Enhanced Vegetation Index (EVI) curves for ecosystem modeling applications. *Remote Sens. Environ.* **2009**, *113*, 2186–2193. [CrossRef]
147. Wu, C.; Chen, J.M.; Huang, N. Predicting gross primary production from the enhanced vegetation index and photosynthetically active radiation: Evaluation and calibration. *Remote Sens. Environ.* **2011**, *115*, 3424–3435. [CrossRef]
148. Liu, H.Q.; Huete, A.R. A feedback based modification of the NDVI to minimize canopy background and atmospheric noise. *IEEE Trans. Geosci. Remote Sens.* **1995**, *33*, 457–465. [CrossRef]
149. Michalak, W.Z. GIS in land use change analysis: Integration of remotely sensed data into GIS. *Appl. Geogr.* **1993**, *13*, 28–44. [CrossRef]
150. Nagendra, H.; Munroe, D.K.; Southworth, J. From pattern to process: Landscape fragmentation and the analysis of land use/land cover change. *Agric. Ecosyst. Environ.* **2004**, *101*, 111–115. [CrossRef]
151. Humacata, L. Análisis espacial de los cambios de usos del suelo. Aplicación con Sistemas de Información Geográfica. *Rev. Cart.* **2019**, *98*, 239–257. [CrossRef]
152. Tadese, M.; Kumar, L.; Koech, R.; Kogo, B.K. Mapping of land-use/land-cover changes and its dynamics in Awash River Basin using remote sensing and GIS. *Remote Sens. Appl. Soc. Environ.* **2020**, *19*, 100352. [CrossRef]
153. Pontius, R.G.; Shusas, E.; McEchern, M. Detecting important categorical land changes while accounting for persistence. *Agric. Ecosyst. Environ.* **2004**, *101*, 251–268. [CrossRef]
154. Pontius, R.G.; Malizia, N.R. Effect of Category Aggregation on Map Comparison. In *GIScience 2004, LNCS 3234*, 1st ed.; Egenhofer, M.J., Freksa, C., Miller, H.J., Eds.; Springer-Verlag: Berlin/Heidelberg, Germany, 2004; pp. 251–268. [CrossRef]
155. Farfán, M.; Rodríguez-Tapia, G.; Mas, J.F. Hierarchical analysis of the intensity of land cover/land use change and deforestation (2000–2008) in the Sierra de Manantlán Biosphere Reserve, México. *Investig. Geográficas* **2016**, *90*, 89–104. [CrossRef]
156. Damián, D.A.; Márquez, C.O.; García, V.J.; Rodríguez, M.V.; Recalde, C.G. Systematic transitions in land use and land cover in a high Andean micro-basin, Ecuador 1991–2011. *Rev. Espac.* **2018**, *39*, 8–20. Available online: <https://www.revistaespacios.com/a18v39n32/18393208.html> (accessed on 5 August 2022).
157. Esteban-Parra, M.J.; Rodrigo, F.S.; Castro-Díez, Y. Spatial and temporal patterns of precipitation in Spain for the period 1880–1992. *Int. J. Climatol.* **1998**, *18*, 1557–1574. [CrossRef]
158. Spinoni, J.; Naumann, G.; Vogt, J.V.; Barbosa, P. The biggest drought events in Europe from 1950 to 2012. *J. Hydrol. Reg. Stud.* **2015**, *3*, 509–524. [CrossRef]
159. Hanel, M.; Rakovec, O.; Markonis, Y.; Máca, P.; Samaniego, L.; Kysely, J.; Kumar, R. Revisiting the recent European droughts from a long-term perspective. *Sci. Rep.* **2018**, *8*, 9499. [CrossRef]
160. Novillo, C.J.; Arrogante-Funes, P.; Romero-Calcerrada, R. Recent NDVI Trends in Mainland Spain: Land-Cover and Phytoclimatic-Type Implications. *ISPRS Int. J. Geo-Inf.* **2019**, *8*, 43. [CrossRef]
161. Martínez-Fernández, J.; Ruiz-Benito, P.; Zavala, M.A. Recent land cover changes in Spain across biogeographical regions and protection levels: Implications for conservation policies. *Land Use Policy* **2015**, *44*, 62–75. [CrossRef]
162. Lasanta, T.; Nadal-Romero, E.; Khorchani, M.; Romero-Díaz, A. A review of abandoned lands in Spain: From local landscapes to global management strategies. *CIG* **2021**, *47*, 477–521. [CrossRef]
163. De Luis, M.; González-Hidalgo, J.C.; Longares, L.A.; Štěpánek, P. Seasonal precipitation trends in the Mediterranean Iberian Peninsula in second half of 20th century. *Int. J. Climatol.* **2009**, *29*, 1312–1323. [CrossRef]
164. Merino, A.; López, L.; Hermida, L.; Sánchez, J.L.; García-Ortega, E.; Gascón, E.; Fernández-González, S. Identification of drought phases in a 110-year record from Western Mediterranean basin: Trends, anomalies, and periodicity analysis for Iberian Peninsula. *Glob. Planet. Chang.* **2015**, *133*, 96–108. [CrossRef]
165. Llasat, M.C.; Quintas, L. Stationarity of monthly rainfall series since the middle of the XIXth Century. Application to the case of Peninsular Spain. *Nat. Hazards* **2004**, *31*, 613–622. [CrossRef]
166. Peña-Gallardo, M.; Gámiz-Fortis, S.R.; Castro-Díez, Y.; Esteban-Parra, M.J. Comparative analysis of drought indices in Andalusia for the period 1901–2012. *Cuad. Investig. Geogr.* **2016**, *42*, 67–88. [CrossRef]
167. García-Barrón, L.; Aguilar, M.; Sousa, A. Evolution of annual rainfall irregularity in the southwest of the Iberian Peninsula. *Theor. Appl. Climatol.* **2011**, *103*, 13–26. [CrossRef]
168. Sousa, P.M.; Trigo, R.M.; Aizpurua, P.; Nieto, R.; Gimeno, L.; Garcia-Herrera, R. Trends and extremes of drought indices throughout the 20th century in the Mediterranean. *Nat. Hazards Earth Syst. Sci.* **2011**, *11*, 33–51. [CrossRef]
169. Paredes, D.; Trigo, R.M.; Garcia-Herrera, R.; Franco-Trigo, I. Understanding Precipitation Changes in Iberia in Early Spring: Weather Typing and Storm-Tracking Approaches. *J. Hydrometeorology* **2006**, *7*, 101–113. Available online: <https://eprints.ucm.es/id/eprint/34761/1/garciaherrera52libre.pdf> (accessed on 24 November 2022). [CrossRef]
170. Aguilar-Alba, M. Recent changes and tendencies in precipitation in Andalusia. In *Climate Change in Andalusia: Evolution and Environmental Consequences*; Ministry of Environment (Junta de Andalucía): Sevilla, Spain, 2007; Volume 1, pp. 99–116. Available online: https://www.juntadeandalucia.es/medioambiente/web/Bloques_Tematicos/Educacion_Y_Participacion_Ambiental/Educacion_Ambiental/el_cambio_climatico_en_andalucia/capitulo5.pdf (accessed on 24 November 2022).
171. Regos, A.; Ninyerola, M.; Moré, G.; Pons, X. Linking land cover dynamics with driving forces in mountain landscape of the Northwestern Iberian Peninsula. *Int. J. Appl. Earth Obs. Geoinf.* **2015**, *38*, 1–14. [CrossRef]
172. Palombo, C.; Chirici, G.; Marchetti, M.; Tognetti, R. Is land abandonment affecting forest dynamics at high elevation in Mediterranean mountains more than climate change? *Plant Biosyst.* **2013**, *147*, 1–11. [CrossRef]

173. IPCC Assessment Reports. Available online: https://www.miteco.gob.es/es/ceneam/recursos/mini-portales-tematicos/Cclimatico/informe_ipcc.aspx (accessed on 25 November 2022).
174. Impacts and Risks Derived from Climate Change in Spain. Available online: https://transparencia.gob.es/transparencia/transparencia_Home/index/MasInformacion/Informes-de-interes/Medio_ambiente/CambioClimatico.html (accessed on 25 November 2022).
175. Local Climate Change Scenarios in Andalusia. Available online: https://www.juntadeandalucia.es/medioambiente/portal/web/cambio-climatico/indice/-/asset_publisher/hdxWUGtQGkX8/content/resultados-de-los-escenarios-locales-cambio-clim-c3-a1tico-actualizados-al-5-c2-ba-informe-ipcc-evoluci-c3-b3n-de-los-grupos-clim-c3-a1ticos-y-la-temp/20151 (accessed on 25 November 2022).
176. Water Accounts. Environment 2011, Number 65. Available online: <https://dialnet.unirioja.es/revista/7639/A/2011> (accessed on 25 November 2022).

Disclaimer/Publisher's Note: The statements, opinions and data contained in all publications are solely those of the individual author(s) and contributor(s) and not of MDPI and/or the editor(s). MDPI and/or the editor(s) disclaim responsibility for any injury to people or property resulting from any ideas, methods, instructions or products referred to in the content.